



GREENBOOK
adapting settlements for the future

DETAILED PROJECTIONS OF FUTURE CLIMATE CHANGE OVER SOUTH AFRICA

WORKSTREAM 2: RESEARCH REPORT

2019



www.greenbook.co.za

Project partner



Funded by



International Development Research Centre
Centre de recherches pour le développement international





Authors	Francois Engelbrecht
Date	2019
ToDB reference	CSIR/BE/SPS/ER/2019/0005/C
Suggested citation	Engelbrecht, F. 2019. <i>Green Book – Detailed Projections of Future Climate Change over South Africa</i> . Technical report, Pretoria: CSIR

Disclaimer and acknowledgement: *This work was carried out with the aid of a grant from the CSIR Long-term Thematic Programme, Pretoria, South Africa and the International Development Research Centre, Ottawa, Canada. The views expressed herein do not necessarily represent those of the IDRC or its Board of Governors.*



TABLE OF CONTENTS

1	INTRODUCTION	7
2	CLIMATE MODEL SIMULATIONS	7
2.1	Experimental design of the regional climate model simulations	7
3	RESULTS	9
3.1	Average temperature	10
3.2	Maximum temperature	15
3.3	Minimum temperatures	19
3.4	Very hot days	23
3.5	Heat-wave days	27
3.6	High fire-danger days	31
3.7	Rainfall	35
3.8	Extreme rainfall events (including severe thunderstorms and lightning)	39
3.9	Wind speed	43
4	CONCLUSIONS	47
5	REFERENCES	48



TABLE OF FIGURES

Figure 1: CCAM simulated annual average temperature (°C) over South Africa at 8 km resolution, for the baseline period 1961-1990. The median of simulations is shown for the ensemble of downscalings of six GCM simulations.	11
Figure 2: CCAM projected change in the annual average temperature (°C) over South Africa at 8 km resolution, for the time-slab 2021-2050 relative to 1961-1990. The 10 th , 50 th and 90 th percentiles are shown for the ensemble of downscalings of six GCM projections	13
Figure 3: CCAM projected change in the annual average temperature (°C) over South Africa at 8 km resolution, for the time-slab 2070-2099 relative to 1961-1990. The 10 th , 50 th and 90 th percentiles are shown for the ensemble of downscalings of six GCM projections	14
Figure 4: CCAM simulated annual average maximum temperature (°C) over South Africa at 8 km resolution, for the baseline period 1961-1990. The median of simulations is shown for the ensemble of downscalings of six GCM simulations.	15
Figure 5: CCAM projected change in the annual average maximum temperature (°C) over South Africa at 8 km resolution, for the time-slab 2021-2050 relative to 1961-1990. The 10 th , 50 th and 90 th percentiles are shown for the ensemble of downscalings of six GCM projections under RCP4.5 (left) and RCP8.5 (right).....	17
Figure 6: CCAM projected change in the annual average maximum temperature (°C) over South Africa at 8 km resolution, for the time-slab 2021-2050 relative to 1961-1990. The 10 th , 50 th and 90 th percentiles are shown for the ensemble of downscalings of six GCM projections under RCP4.5 (left) and RCP8.5 (right).....	18
Figure 7: CCAM simulated annual average minimum temperature (°C) over South Africa at 8 km resolution, for the baseline period 1961-1990. The median of simulations is shown for the ensemble of downscalings of six GCM simulations	19
Figure 8: CCAM projected change in the annual average minimum temperature (°C) over South Africa at 8 km resolution, for the time-slab 2021-2050 relative to 1961-1990. The 10 th , 50 th and 90 th percentiles are shown for the ensemble of downscalings of six GCM projections under RCP4.5 (left) and RCP8.5 (right).....	21
Figure 9: CCAM projected change in the annual average minimum temperature (°C) over South Africa at 8 km resolution, for the time-slab 2070-2099 relative to 1961-1990. The 10 th , 50 th and 90 th percentiles are shown for the ensemble of downscalings of six GCM projections under RCP4.5 (left) and RCP8.5 (right).....	22
Figure 10: CCAM simulated annual average number of very hot days (units are number of days per grid point per year) over South Africa at 8 km resolution, for the baseline period 1961-1990. The median of simulations is shown for the ensemble of downscalings of six GCM simulations.....	23



Figure 11: CCAM projected change in the annual average number of very hot days (units are days per grid point per year) over South Africa at 8 km resolution, for the time-slab 2021-2050 relative to 1961-1990. The 10th, 50th and 90th percentiles are shown for the ensemble of downscalings of six GCM projections under RCP4.5 (left) and RCP8.5 (right). 25

Figure 12: CCAM projected change in the annual average number of very hot days (units are days per grid point per year) over South Africa, for the time-slab 2071-2100 relative to 1961-1990. The 10th, 50th and 90th percentiles are shown for the ensemble of downscalings of six GCM projections under RCP4.5 (left) and RCP8.5 (right). 26

Figure 13: CCAM simulated annual average number of heat-wave days (units are number of days per grid point per year) over South Africa at 8 km resolution, for the baseline period 1961-1990. The median of simulations is shown for the ensemble of downscalings of six GCM simulations. 27

Figure 14: CCAM projected change in the annual average number of heat-wave days (units are number of days per grid point per year) over South Africa, for the time-slab 2021-2050 relative to 1961-1990. The 10th, 50th and 90th percentiles are shown for the ensemble of downscalings of six GCM projections under RCP4.5 (left) and RCP8.5 (right). 29

Figure 15: CCAM projected change in the annual average number of heat-wave days (units are number of days per grid point per year) over South Africa, for the time-slab 2071-2100 relative to 1961-1990. The 10th, 50th and 90th percentiles are shown for the ensemble of downscalings of six GCM projections under RCP4.5 (left) and RCP8.5 (right). 30

Figure 16: CCAM simulated annual average number of high fire-danger days (units are number of days per grid point per year) over South Africa, for the baseline period 1961-1990. The median of simulations is shown for the ensemble of downscalings of six GCM simulations. 31

Figure 17: CCAM projected change in the annual average number of high fire-danger days (units are number of days per grid point per year) over South Africa, for the time-slab 2021-2050 relative to 1961-1990. The 10th, 50th and 90th percentile are shown for the ensemble of downscalings of six GCM projections under RCP4.5 (left) and RCP8.5 (right). 33

Figure 18: CCAM projected change in the annual average number of high fire-danger days (units are number of days per grid point per year) over South Africa, for the time-slab 2071-2100 relative to 1961-1990. The 10th, 50th and 90th percentile are shown for the ensemble of downscalings of six GCM projections under RCP4.5 (left) and RCP8.5 (right). 34

Figure 19: CCAM simulated annual average rainfall totals (mm) over eastern South Africa, for the baseline period 1961-1990 at 8 km resolution. The median of simulations is shown for the ensemble of downscalings of six GCM simulations. 35



Figure 20: CCAM projected change in the annual average rainfall totals (mm) over eastern South Africa at 8 km resolution, for the time-slab 2021-2050 relative to 1961-1990. The 10th, 50th and 90th percentiles are shown for the ensemble of downscalings of six GCM projections under RCP4.5 (left) and RCP8.5 (right)..... 37

Figure 21: CCAM projected change in the annual average rainfall totals (mm) over eastern South Africa, for the time-slab 2071-2100 relative to 1961-1990. The 10th, 50th and 90th percentiles are shown for the ensemble of downscalings of six GCM projections under RCP4.5 (left) and RCP8.5 (right). 38

Figure 22: CCAM simulated annual average number of extreme rainfall days (units are number of days per grid point per year) over South Africa, for the baseline period 1961-1990. The median of simulations is shown for the ensemble of downscalings of six GCM simulations. 39

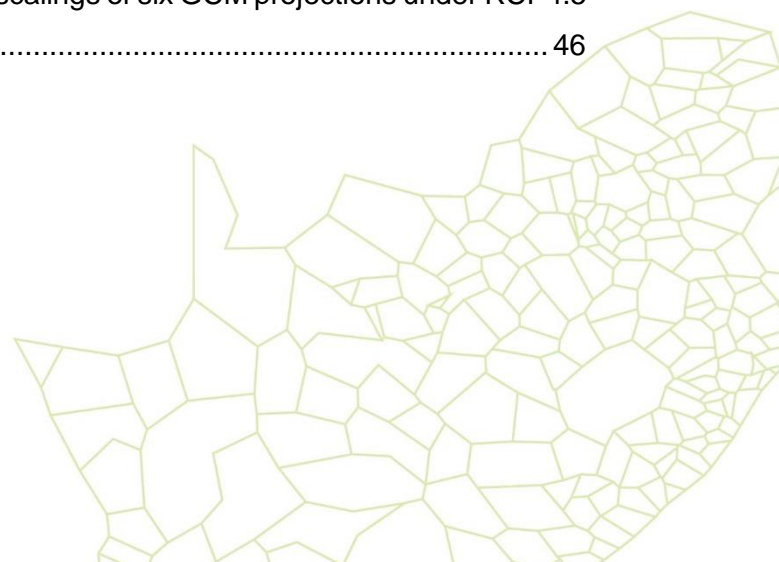
Figure 23: CCAM projected change in the annual average number of extreme rainfall days (units are numbers of grid points per year) over South Africa at 8 km resolution, for the time-slab 2021-2050 relative to 1961-1990. The 10th, 50th and 90th percentiles are shown for the ensemble of downscalings of six GCM projections under RCP4.5 (left) and RCP8.5 (right).41

Figure 24: CCAM projected change in the annual average number of extreme rainfall days (units are numbers of grid points per year) over eastern South Africa, for the time-slab 2071-2100 relative to 1961-1990. The 10th, 50th and 90th percentiles are shown for the ensemble of downscalings of six GCM projections under RCP4.5 (left) and RCP8.5 (right). 42

Figure 25: CCAM simulated average annual wind speed (m/s) over South Africa at 8 km resolution, for the baseline period 1961-1990. The median of simulations is shown for the ensemble of downscalings of six GCM simulations. 43

Figure 26: CCAM projected change in the annual average wind speed (m/s) over South Africa at 8 km resolution, for the time-slab 2021-2050 relative to 1961-1990. The 10th, 50th and 90th percentiles are shown for the ensemble of downscalings of six GCM projections under RCP4.5 (left) and RCP8.5 (right) 45

Figure 27: CCAM projected change in the annual average wind speed (m/s) over South Africa at 8 km resolution, for the time-slab 2091-2100 relative to 1961-1990. The 10th, 50th and 90th percentiles are shown for the ensemble of downscalings of six GCM projections under RCP4.5 (left) and RCP8.5 (right). 46





1 INTRODUCTION

Climate change is projected to impact drastically in southern African during the 21st century under low mitigation futures (Niang et al., 2014). African temperatures are projected to rise rapidly, at 1.5 to 2 times the global rate of temperature increase (James and Washington, 2013; Engelbrecht et al., 2015). Moreover, the southern African region is projected to become generally drier under enhanced anthropogenic forcing (Christensen et al., 2007; Engelbrecht et al., 2009; James and Washington, 2013; Niang et al., 2014). These changes will plausibly have a range of impacts on the South African environment and economy, including impacts on energy demand (in terms of achieving human comfort within buildings and factories), water security (through reduced rainfall and enhanced evapotranspiration) and agriculture (in terms of changes in crop yield) (Engelbrecht et al., 2015).

However, climate change impacts are not to manifest only through changes in average temperature and rainfall patterns, but also through changes in the attributes of extreme weather events. For the southern African region, generally drier conditions and the more frequent occurrence of dry spells are plausible over most of the interior (Christensen et al., 2007; Engelbrecht et al., 2009). Tropical cyclone tracks are projected to shift northward, bringing more flood events to northern Mozambique and fewer to the Limpopo province in South Africa (Malherbe et al., 2013). Cut-off low related flood events are also projected to occur less frequently over South Africa (Engelbrecht et al., 2013) in response to a poleward displacement of the westerly wind regime. Intense thunderstorms are plausible to occur more frequently over South Africa in a generally warmer climate (Engelbrecht et al., 2013). The purpose of this project is to provide new insights and evidence regarding future changes in the frequency of occurrence of extreme events over southern Africa, with a focus on extreme events that impact directly on South African cities. This is achieved through the analysis of a set of very high resolution projections of future climate change.

2 CLIMATE MODEL SIMULATIONS

2.1 Experimental design of the regional climate model simulations

An ensemble of very high resolution climate model simulations of present-day climate and projections of future climate change over South Africa has been performed as part of the



project research. These simulations were subsequently described to illustrate how climate change is to impact on the occurrence of extreme events and renewable energy potential of the country. The regional climate model used is the conformal-cubic atmospheric model (CCAM), a variable-resolution global climate model (GCM) developed by the Commonwealth Scientific and Industrial Research Organisation (CSIRO) (McGregor 2005; McGregor and Dix 2001, 2008). CCAM runs coupled to a dynamic land-surface model CABLE (CSIRO Atmosphere Biosphere Land Exchange model). Six GCM simulations of the Coupled Model Intercomparison Project Phase Five (CMIP5) and Assessment Report Five (AR5) of the Intergovernmental Panel on Climate Change (IPCC), obtained for the emission scenarios described by Representative Concentration Pathways 4.5 and 8.5 (RCP4.5 and 8.5) were first downscaled to 50 km resolution globally. The simulations span the period 1960-2100. RCP4.5 is a high mitigation scenario, whilst RCP8.5 is a low mitigation scenario. The GCMs downscaled include the Australian Community Climate and Earth System Simulator (ACCESS1-0); the Geophysical Fluid Dynamics Laboratory Coupled Model (GFDL-CM3); the National Centre for Meteorological Research Coupled Global Climate Model, version 5 (CNRM-CM5); the Max Planck Institute Coupled Earth System Model (MPI-ESM-LR); the Norwegian Earth System Model (NorESM1-M) and the Community Climate System Model (CCSM4). The simulations were performed on supercomputers of the Centre for High Performance Computing (CHPC) of the Meraka Institute of the CSIR in South Africa. In these simulations CCAM was forced with the bias-corrected daily sea-surface temperatures (SSTs) and sea-ice concentrations of each host model, and with CO₂, sulphate and ozone forcing consistent with the RCP4.5 and RCP8.5 scenarios. The model's ability to realistically simulate present-day southern African climate has been extensively demonstrated (e.g. Engelbrecht et al., 2009; Engelbrecht et al., 2011; Engelbrecht et al., 2012; Malherbe et al., 2013; Winsemius et al., 2014; Engelbrecht et al., 2015). Most current coupled GCMs do not employ flux corrections between atmosphere and ocean, which contributes to the existence of biases in their simulations of present-day sea-surface temperatures (SSTs) – more than 2°C along the West African coast. An important feature of the downscalings performed here is that the model was forced with the bias-corrected SSTs and sea-ice fields of the GCMs. The bias is computed by subtracting for each month the Reynolds (1988) SST climatology (for 1961-2000) from the corresponding CGCM climatology. The bias-correction is applied consistently throughout the simulation. Through this procedure the climatology of the SSTs applied as lower boundary forcing is the same as that of the Reynolds SSTs. However, the intra-annual variability and climate-change signal of the CGCM SSTs are preserved (Katzfey et al., 2009).



A multiple-nudging strategy was followed to obtain the 8 km resolution downscalings. After completion of the 50 km resolution simulations described above CCAM was integrated in stretched-grid mode over South Africa, at a resolution of about 8 km (0.08° degrees in latitude and longitude). The high resolution part of the model domain was about 2000 x 2000 km² in size. The higher resolution simulations were nudged within the quasi-uniform global simulations, through the application of a digital filter using a 600 km length scale. The filter was applied at six-hourly intervals and from 900 hPa upwards.

3 RESULTS

The model integrations performed at a resolution of 8 km over South Africa offer a number of advantages over the 50 km resolution simulations. Firstly, convective rainfall is partially resolved in the 8 km simulations, implying that the model is less dependent on statistics to simulate this intricate aspect of the atmospheric dynamics and physics. Secondly, important topographic features such the southern and eastern escarpments are much better resolved in the 8 km resolution simulations, implying that the topographic forcing of temperatures, wind patterns and convective rainfall can be simulated more realistically. The 8 km resolution results represented here may therefore be regarded as providing a new and authoritative view on the futures of extreme weather events over South Africa under climate change. In this section the projected changes in a number of climatological variables, including extreme weather-events metrics, are presented. For each of the metrics under consideration, the simulated baseline (climatological) state over South Africa calculated for the period 1961-1990 is shown in a first figure (note that the median of the six downscalings is shown in this case). The projected changes in the metric are subsequently shown, for the time-slab 2021-2050 relative to the baseline period 1961-2000, first for RCP8.5 (low mitigation) and then for RCP4.5 (high mitigation). Three figures are presented for each metric for each RCP, for the 10th, 50th (median) and 90th percentiles of the ensemble of projected changes under the RCP. In this way, it is possible to gain some understanding of the uncertainty range that is associated with the projections. Finally, the projections are shown for the region 35 °S to 22 °S and 16 °E to 33 °E, that is, for a domain covering the entire South Africa at 8 km resolution. A list of the climate metrics analysed in this report is provided in Table 1.



Table 1: Relevant climate variables

Variable	Description and/or units
Average temperature	°C
Minimum temperature	°C
Maximum temperature	°C
Very hot days	A day when the maximum temperature exceeds 35 °C. Units are number of events per grid point per year.
Heat-wave days	The maximum temperature exceeds the average temperature of the warmest month of the year by 5 °C for at least 3 days.
High fire-danger days	McArthur fire-danger index exceeds a value of 24. Units are number of events per grid point per year.
Rainfall	mm
Extreme rainfall (also a proxy for lightning)	More than 20 mm of rain falling within 24 hrs over an area of 64 km ² . The occurrence of extreme convective rainfall is used as a proxy for the occurrence of storms that produce lightning. Units are number of events per grid point per year.
Wind speed	m/s

3.1 Average temperature

The model-simulated annual average temperatures (°C) are displayed in Figure 1 for the baseline period 1961-1990. The coolest conditions occur over the eastern escarpment regions of the domain. The hottest regions are the east coast, Lowveld, western interior (including the Orange River basin) and the Limpopo River basin.

Rapid rises in the annual-average near-surface temperatures are projected to occur over southern Africa during the 21st century – temperatures over the South African interior are projected to rise at about 1.5 to 2 times the global rate of temperature increase (Engelbrecht et al., 2015).

tave 50 perc

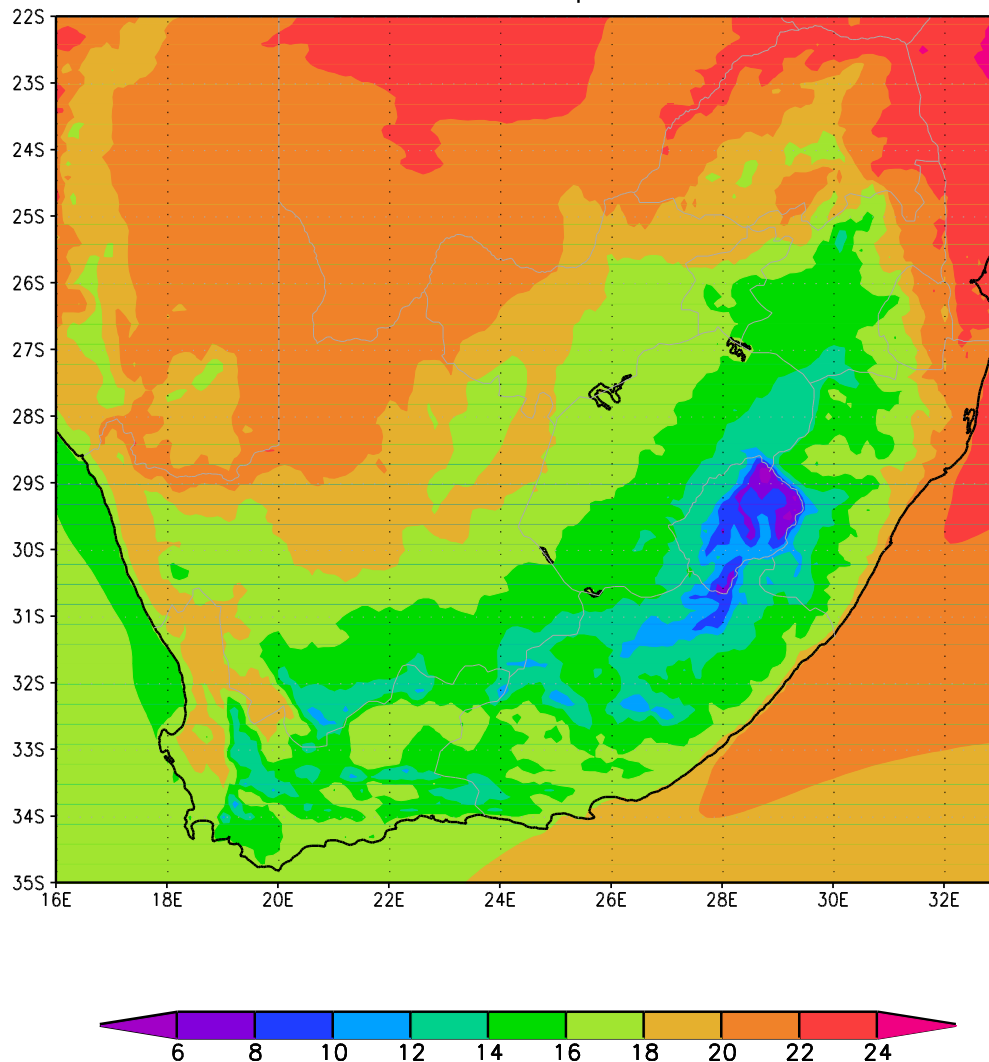


Figure 1: CCAM simulated annual average temperature (°C) over South Africa at 8 km resolution, for the baseline period 1961-1990. The median of simulations is shown for the ensemble of downscalings of six GCM simulations.

For the period 2021-2050 relative to the period 1961-1990, under low mitigation, temperature increases of 1 to 2.5 °C may plausibly occur over the southern coastal regions. Over the interior regions larger temperature increases are likely, which may well exceed 3 °C over the northern parts (Figure 2).

For the period 2070-2099 relative to the period 1961-1990 under low mitigation, temperature increases of 2-3 °C are plausible to occur over the southern coastal regions (Figure 3). Over the interior temperature increases of more than 4 °C are likely, and may well exceed 7 °C over the northern interior. Such drastic temperature increases would have significant impacts on



numerous sectors, including agriculture, water and energy. Under modest-high mitigation, temperature increases may still be significantly reduced, plausibly to less than 2-4 °C even over the interior – with only a minority of downscalings indicative of temperature increases exceeding 4 °C over the northern interior. Under modest-high mitigation, temperature increases over South Africa will be somewhat less, but may still reach 3 °C over the northern interior (Figure 2).

For the period 2070-2099 relative to the period 1961-1990 under low mitigation, temperature increases of 2-3 °C are plausible to occur over the southern coastal regions (Figure 3). Over the interior temperature increases of more than 4 °C are likely, and may well exceed 7 °C over the northern interior. Such drastic temperature increases would have significant impacts on numerous sectors, including agriculture, water and energy. Under modest-high mitigation, temperature increases may still be significantly reduced, plausibly to less than 2-4 °C even over the interior – with only a minority of downscalings indicative of temperature increases exceeding 4 °C over the northern interior. Increasing average temperatures over South Africa may plausibly increase the household demand for cooling over the coming decades.

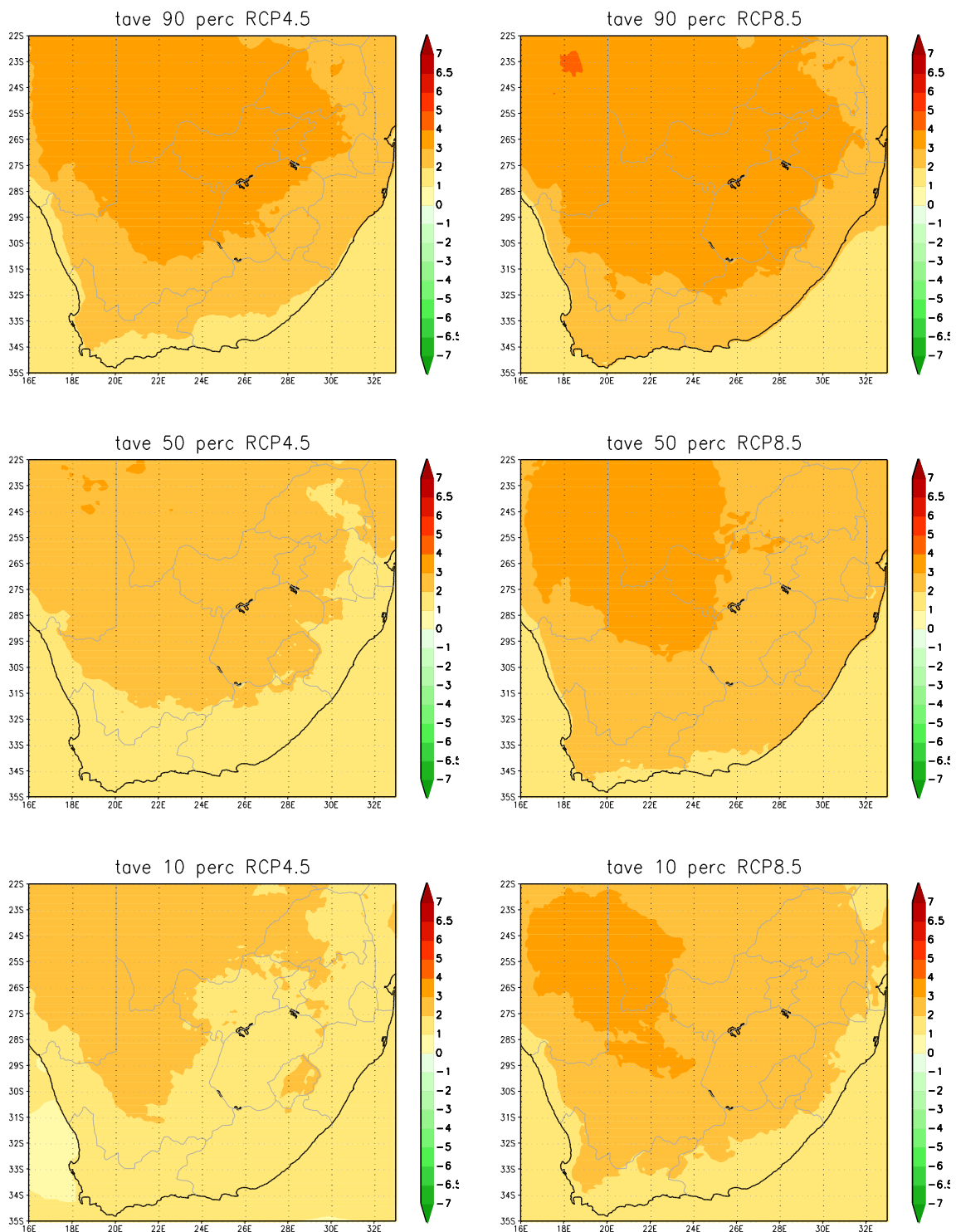


Figure 2: CCAM projected change in the annual average temperature (°C) over South Africa at 8 km resolution, for the time-slab 2021-2050 relative to 1961-1990. The 10th, 50th and 90th percentiles are shown for the ensemble of downscalings of six GCM projections

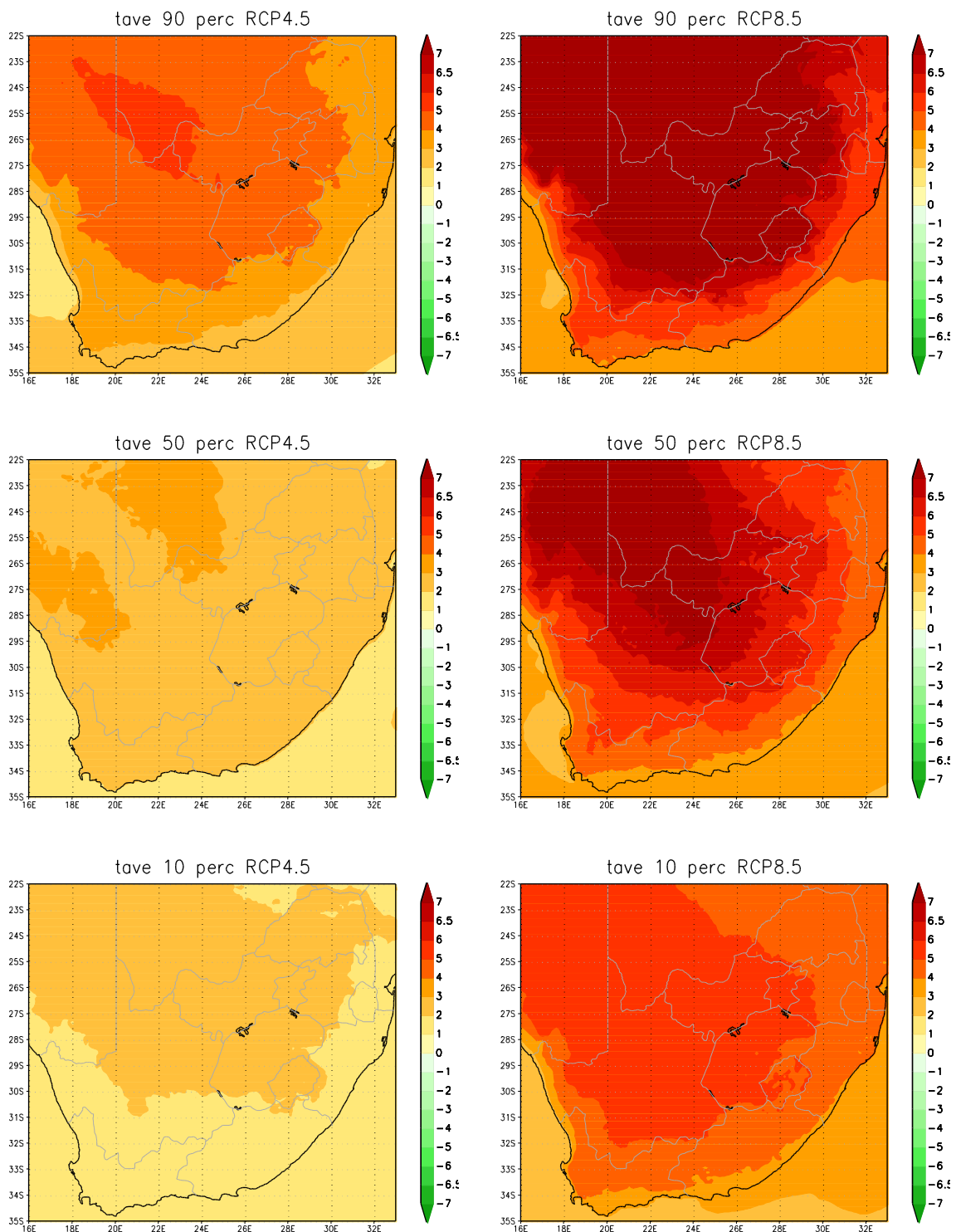


Figure 3: CCAM projected change in the annual average temperature (°C) over South Africa at 8 km resolution, for the time-slab 2070-2099 relative to 1961-1990. The 10th, 50th and 90th percentiles are shown for the ensemble of downscalings of six GCM projections

3.2 Maximum temperature

The model-simulated and bias-corrected annual average maximum temperatures (°C) are displayed in Figure 4 for the baseline period 1961-1990. The lowest maximum temperatures occur over Lesotho. The hottest regions are the Limpopo River basin, the Lowveld and the Northern Cape.

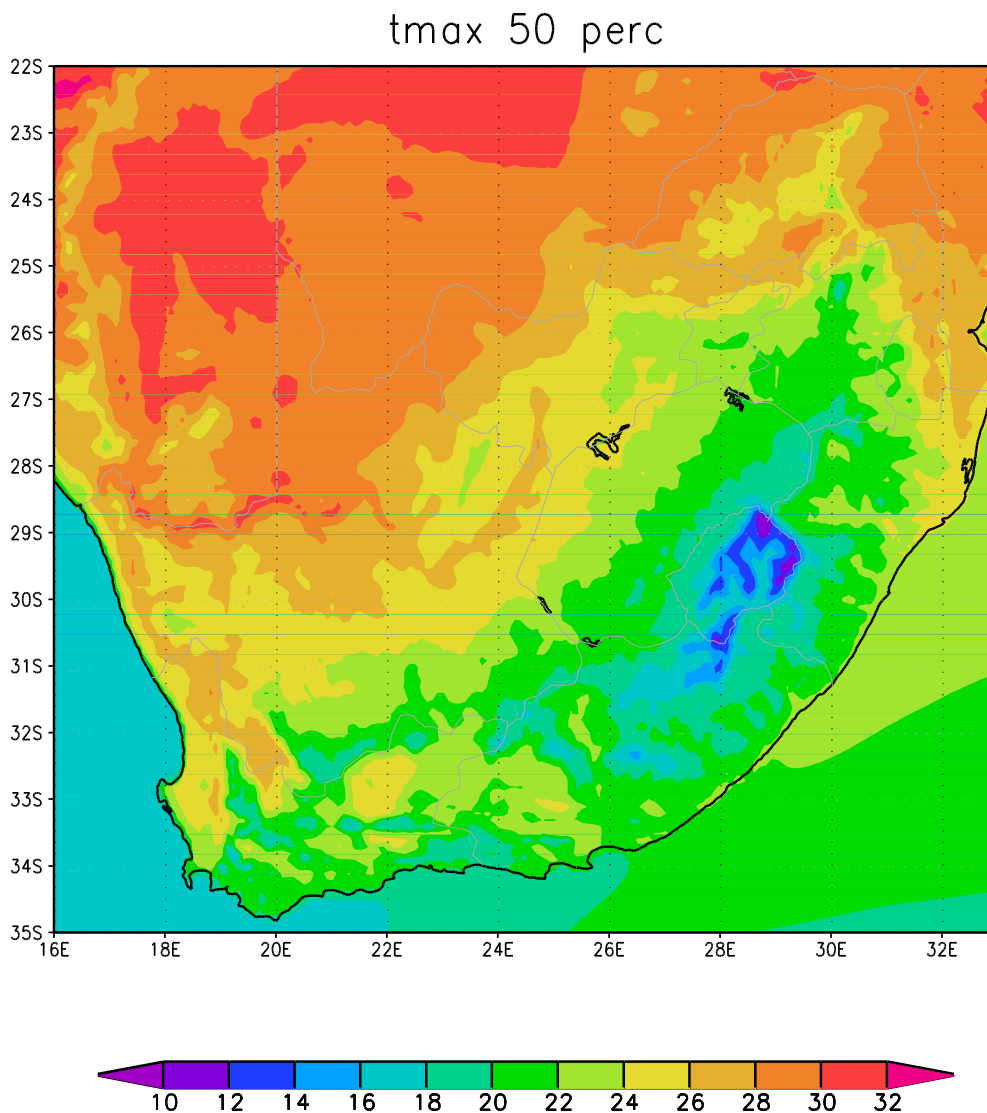


Figure 4: CCAM simulated annual average maximum temperature (°C) over South Africa at 8 km resolution, for the baseline period 1961-1990. The median of simulations is shown for the ensemble of downscalings of six GCM simulations.



Rapid rises in the annual average maximum temperature are projected to occur over southern Africa during the 21st century – temperatures over the South African interior are projected to rise at about twice the global rate of temperature increase. For the period 2021-2050 relative to the period 1961-1990, maximum temperature increases may 3 °C over much of the northern interior of South Africa (Figure 5), with smaller increases plausible over the southern parts (less than 2 °C over the Cape south coast). Under modest-high mitigation, maximum temperature increases over South Africa will be very similar for the mid-future compared to the low mitigation case (Figure 5).

For the period 2070-2099 relative to the period 1961-1990, maximum temperature increases are projected to exceed 4 °C over most of the interior (Figure 6), and may indeed exceed 7 °C over parts of the northern interior. Under modest-high mitigation maximum temperature increases may still reach 4 °C over parts of the northern interior (Figure 6), but the temperature increases are in general significant less than for the low mitigation case. Under both low and high mitigation, maximum temperatures are projected to rise faster than minimum temperatures.

The projected drastic temperature increases under particularly low mitigation may have significant impacts on many sectors, including agriculture (e.g. crop yield and livestock mortality rates), energy demand (an increased need for cooling to achieve human comfort is plausible, particularly in summer) and possibly also on water security (through increased evaporation rates).

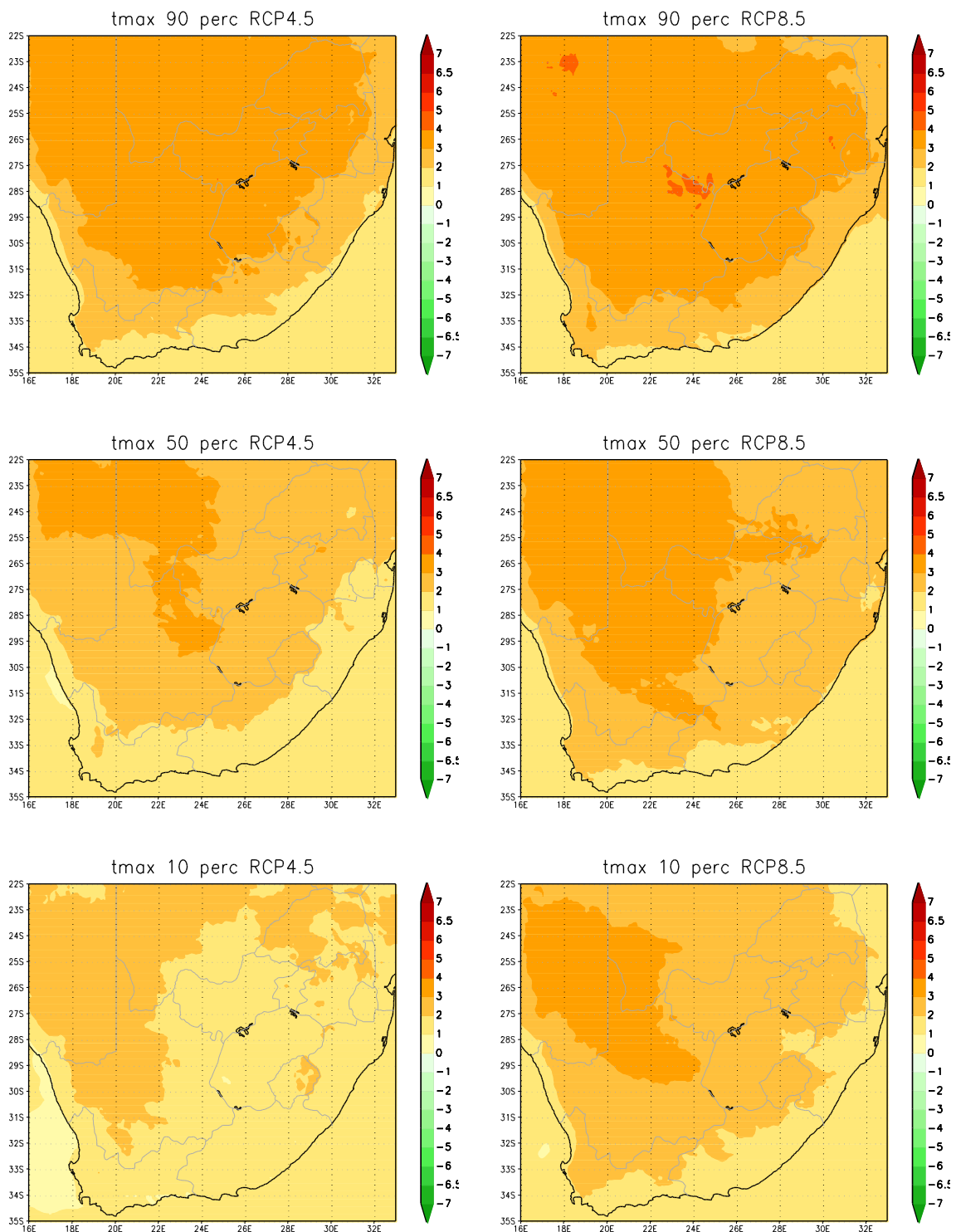


Figure 5: CCAM projected change in the annual average maximum temperature (°C) over South Africa at 8 km resolution, for the time-slab 2021-2050 relative to 1961-1990. The 10th, 50th and 90th percentiles are shown for the ensemble of downscalings of six GCM projections under RCP4.5 (left) and RCP8.5 (right).

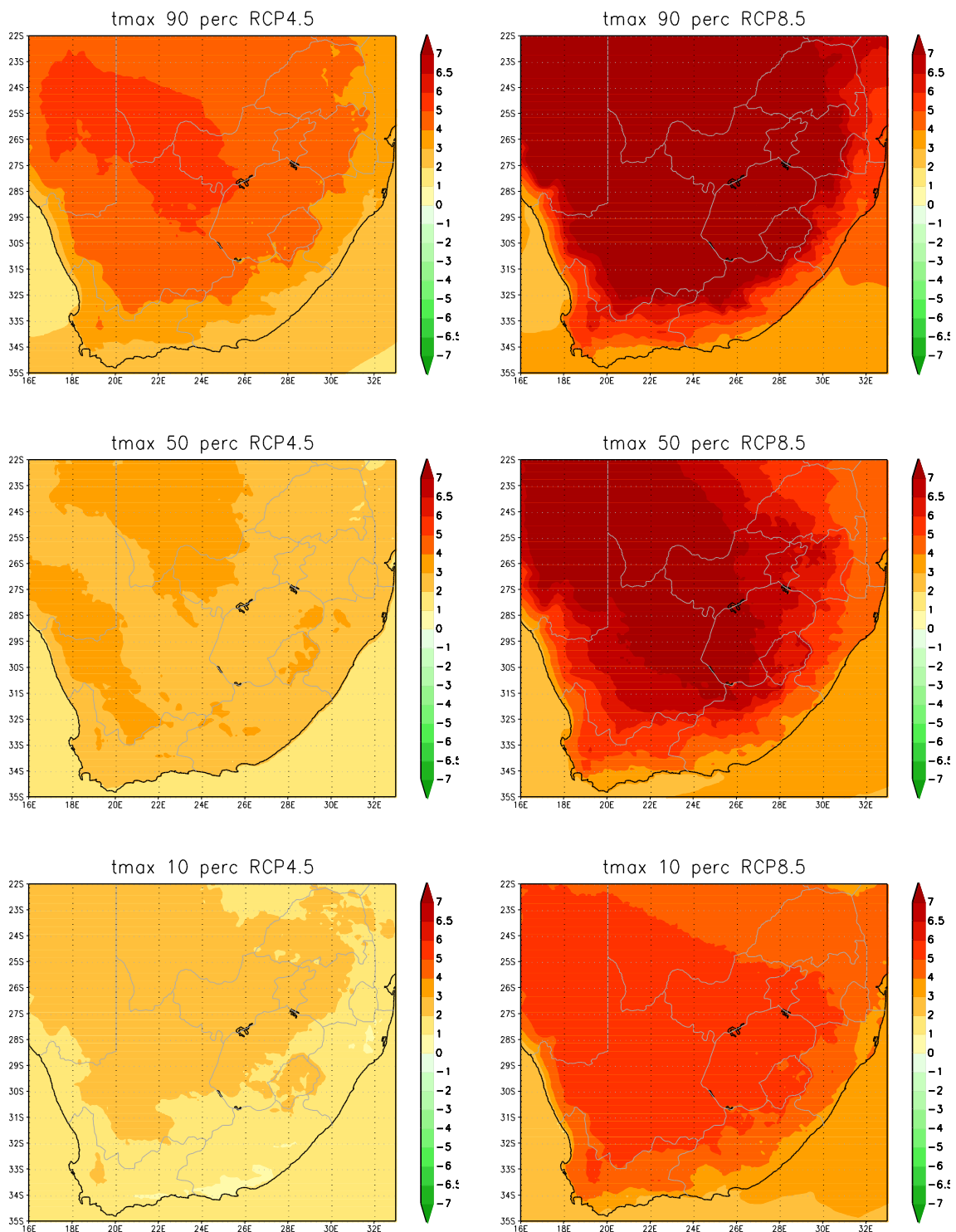


Figure 6: CCAM projected change in the annual average maximum temperature (°C) over South Africa at 8 km resolution, for the time-slab 2021-2050 relative to 1961-1990. The 10th, 50th and 90th percentiles are shown for the ensemble of downscalings of six GCM projections under RCP4.5 (left) and RCP8.5 (right).

3.3 Minimum temperatures

The model-simulated and bias-corrected annual average minimum temperatures (°C) are displayed in Figure 7 for the baseline period 1961-1990. The coolest conditions occur over the escarpment regions of eastern South Africa. The regions with the highest minimum temperatures are the east coast, Lowveld and the Limpopo basin.

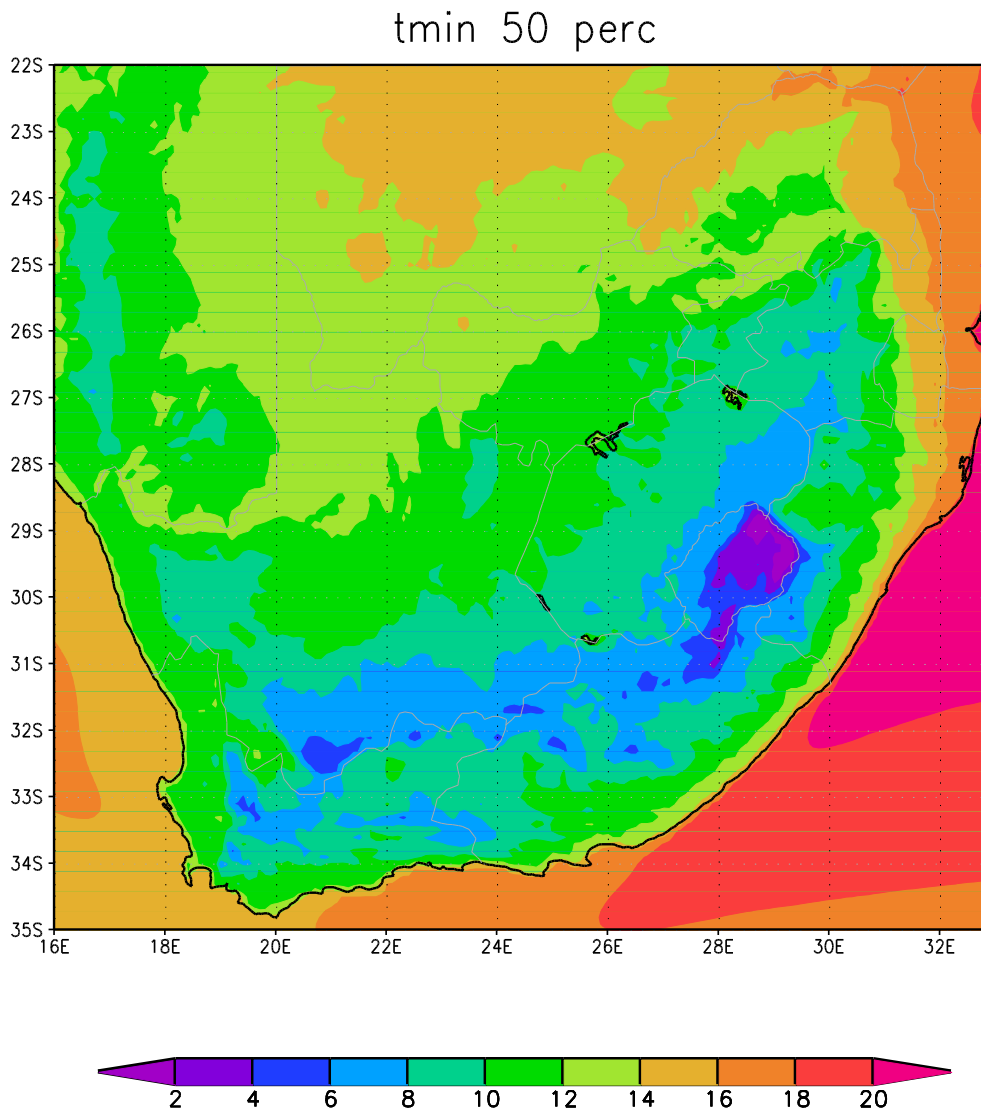


Figure 7: CCAM simulated annual average minimum temperature (°C) over South Africa at 8 km resolution, for the baseline period 1961-1990. The median of simulations is shown for the ensemble of downscalings of six GCM simulations



Rapid rises in the annual average minimum temperature are projected to occur over southern Africa during the 21st century – minimum temperatures over the South African interior are projected to rise at about 1.5 to 2 times the global rate of temperature increase.

For the period 2021-2050 relative to the period 1961-1990, minimum temperature increases of 2 to 3 °C are projected to occur over South Africa under low mitigation (Figure 8). Under high mitigation, minimum temperature increases over South Africa are projected to be very similar to those for the low mitigation case, except along the south and east coast regions where smaller increases are plausible (Figure 8).

For the period 2071-2099 relative to the period 1961-1990, minimum temperature increases of more than 4 °C are projected to occur over much of the interior under low mitigation (Figure 9). These increases may well exceed 7 °C over parts of the northern interior. Smaller changes are projected only for the southern coastal regions. Under modest-high mitigation, minimum temperature increases may likely be reduced to less than 3 °C over much of South Africa, although a minority of downscalings still indicates increases as high as 4 °C over the northern interior (Figure 9).

The projected minimum temperature increases may have significant impacts on energy demand – that is, the household demand for energy during winter (warming need) may be expected to decrease. Rising minimum temperatures are also associated with a decrease in the number of days with frost, with implications for agriculture and bush encroachment.

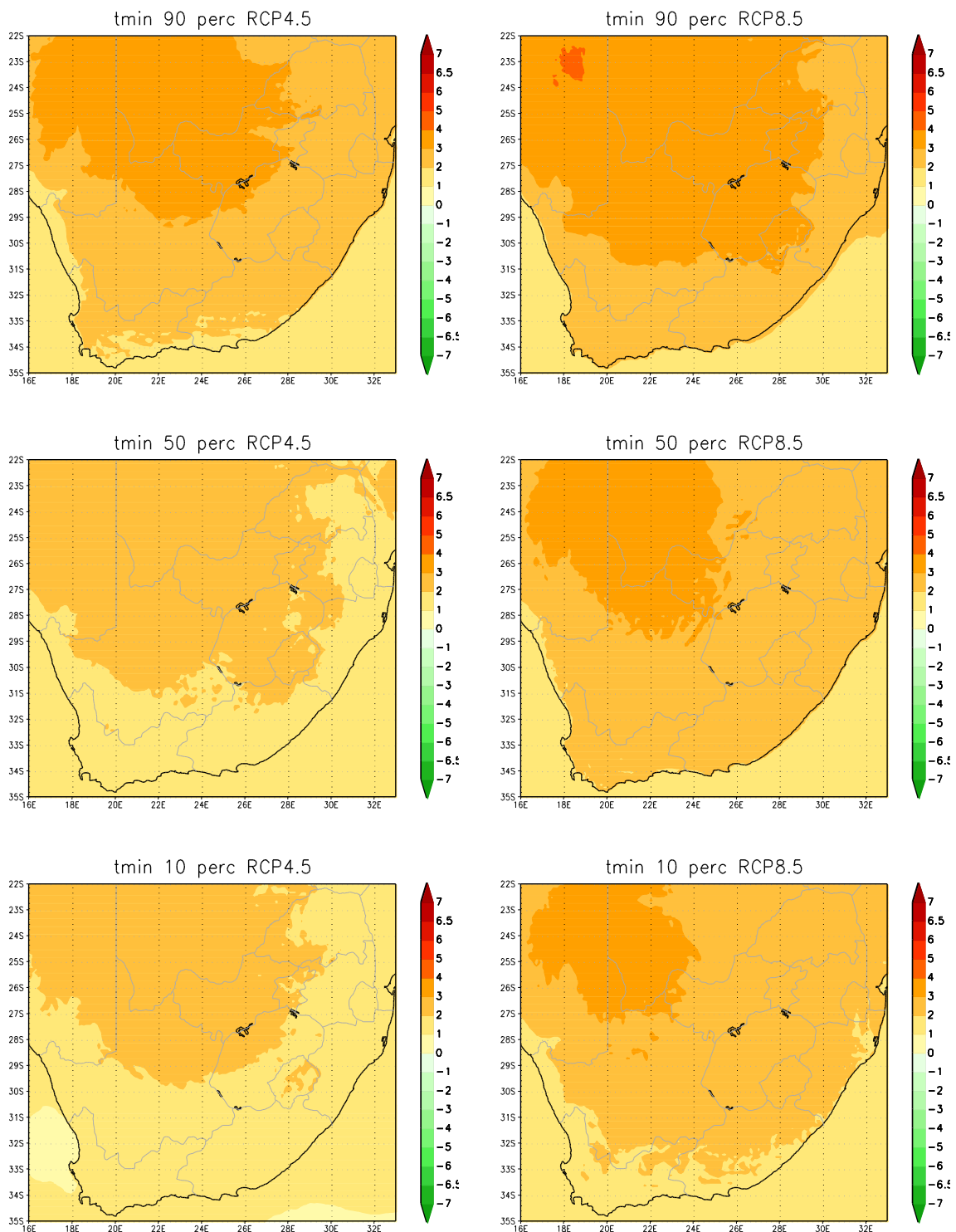


Figure 8: CCAM projected change in the annual average minimum temperature (°C) over South Africa at 8 km resolution, for the time-slab 2021-2050 relative to 1961-1990. The 10th, 50th and 90th percentiles are shown for the ensemble of downscalings of six GCM projections under RCP4.5 (left) and RCP8.5 (right).

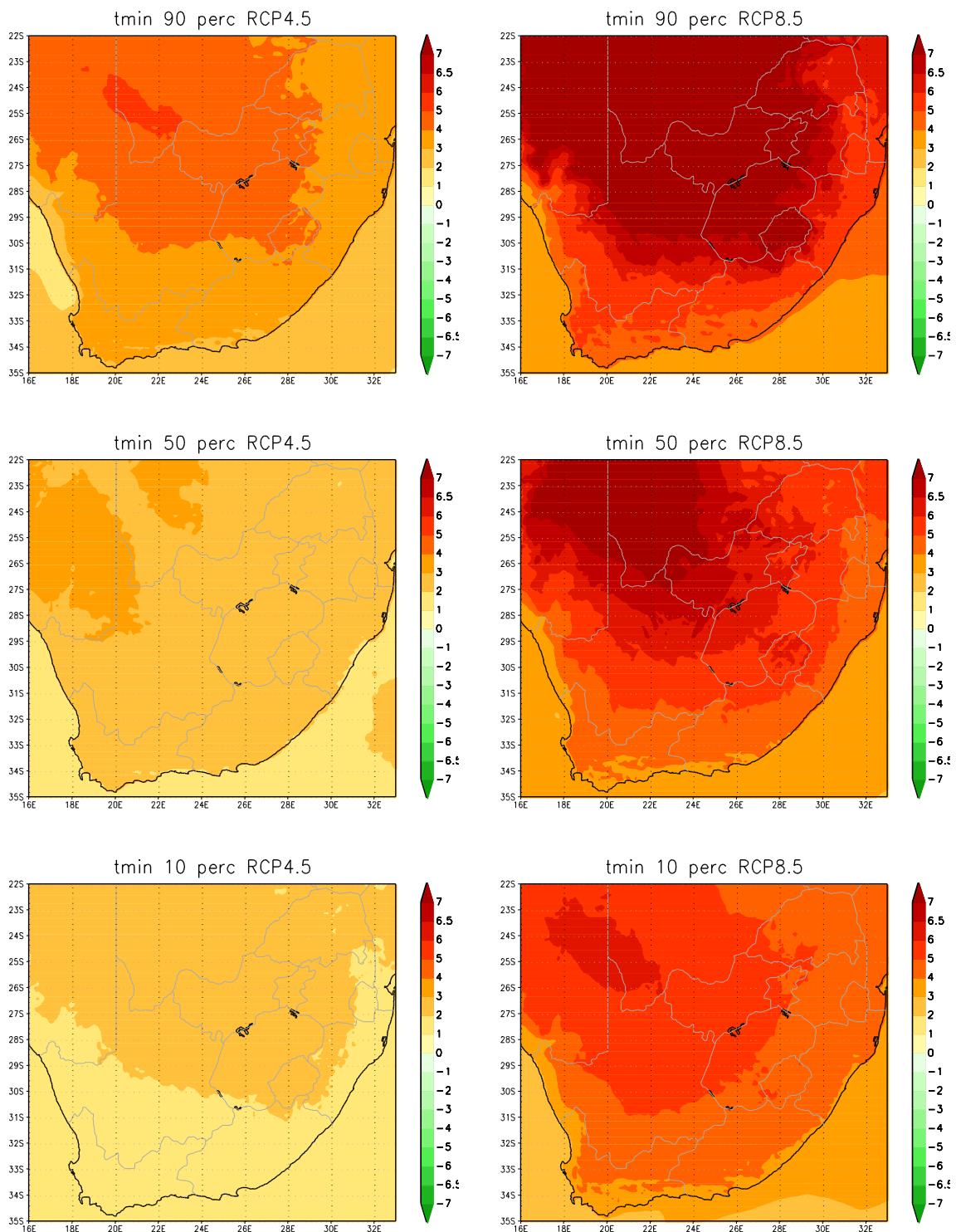


Figure 9: CCAM projected change in the annual average minimum temperature (°C) over South Africa at 8 km resolution, for the time-slab 2070-2099 relative to 1961-1990. The 10th, 50th and 90th percentiles are shown for the ensemble of downscalings of six GCM projections under RCP4.5 (left) and RCP8.5 (right).

3.4 Very hot days

The model-simulated and bias-corrected annual average number of very hot days (days when the maximum temperature exceeds 35 °C - units are number of days per model grid point) are displayed in Figure 10, for the baseline period 1961-1990. In the Limpopo River basin, 60-80 very hot days occur on average annually, with more than 110 such days simulated to occur annually in parts of the Orange River valley.

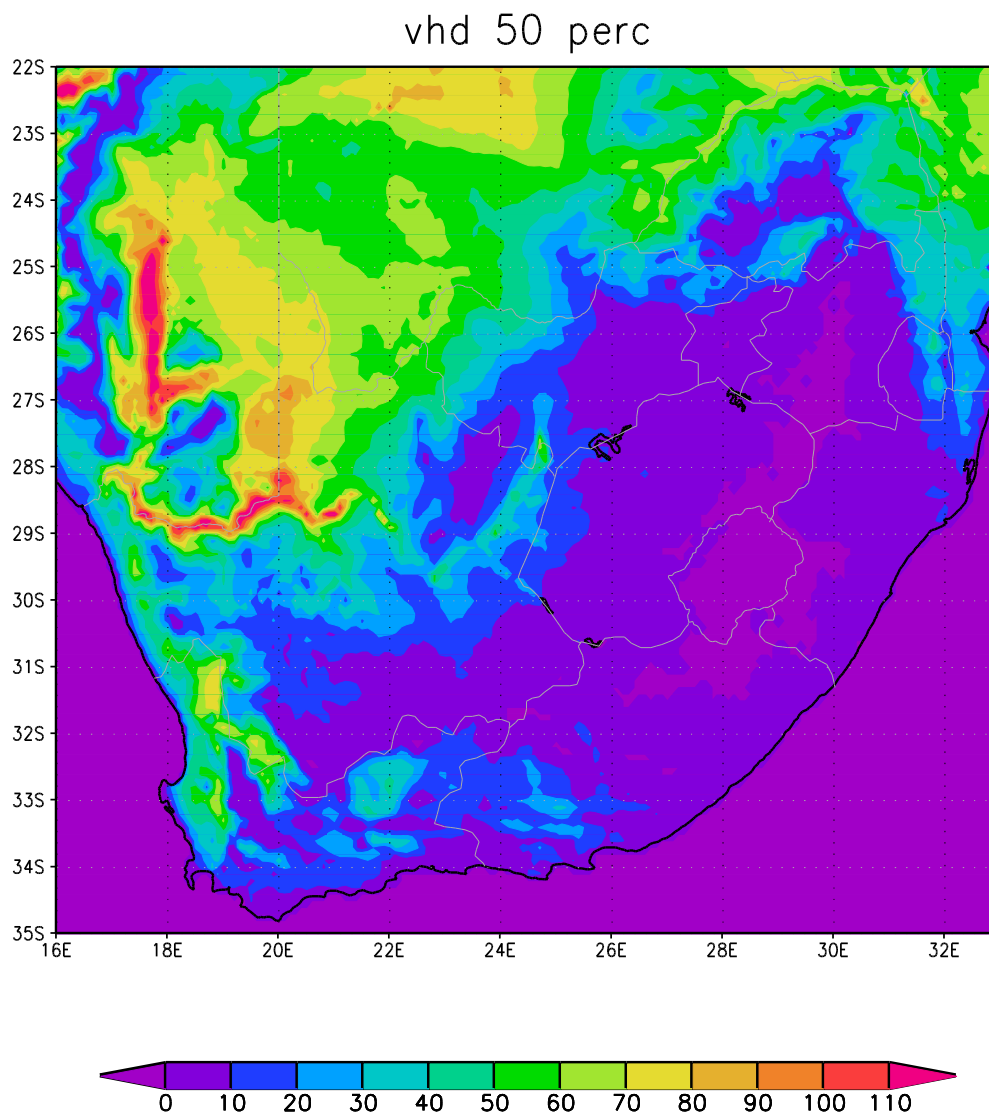


Figure 10: CCAM simulated annual average number of very hot days (units are number of days per grid point per year) over South Africa at 8 km resolution, for the baseline period 1961-1990. The median of simulations is shown for the ensemble of downscalings of six GCM simulations.

In association with drastically rising maximum temperatures (Figures 5 and 6), the frequency of occurrence of very hot days is also projected to increase drastically under climate change. For the period 2021-2050 relative to 1961-1990, under low mitigation, very hot days are



projected to increase with as many as 40-60 days per year in the Limpopo River valley (Figure 11). For the northern parts of the Northern Cape and North West, including the Orange River valley, even larger increases (70 days per year) are projected. More modest increases are projected for the southern interior regions. Even under high mitigation, the increase in the number of very hot days may be as high as 40-50 over the Limpopo River basin and the Orange River valley (Figure 11).

For the period 2070-2099 relative to 1961-1990, under low mitigation, very hot days are projected to increase with 80 days or more per year over the entire northern and western interior of South Africa (Figure 12) – a drastic and potentially devastating increase. Even under high mitigation, the increase in the number of very hot days may be as high as 40-80 over the western and northern interior (Figure 12).

Increases in the occurrence of very hot days occur in association with projected changes in the frequency of occurrence of heat-wave days and high fire-danger days (see sections 3.5 and 3.6). These changes may impact on human and animal health through increased heat stress, are likely to impact negatively on crop yield and are conducive to the occurrence of veld and forest fires.

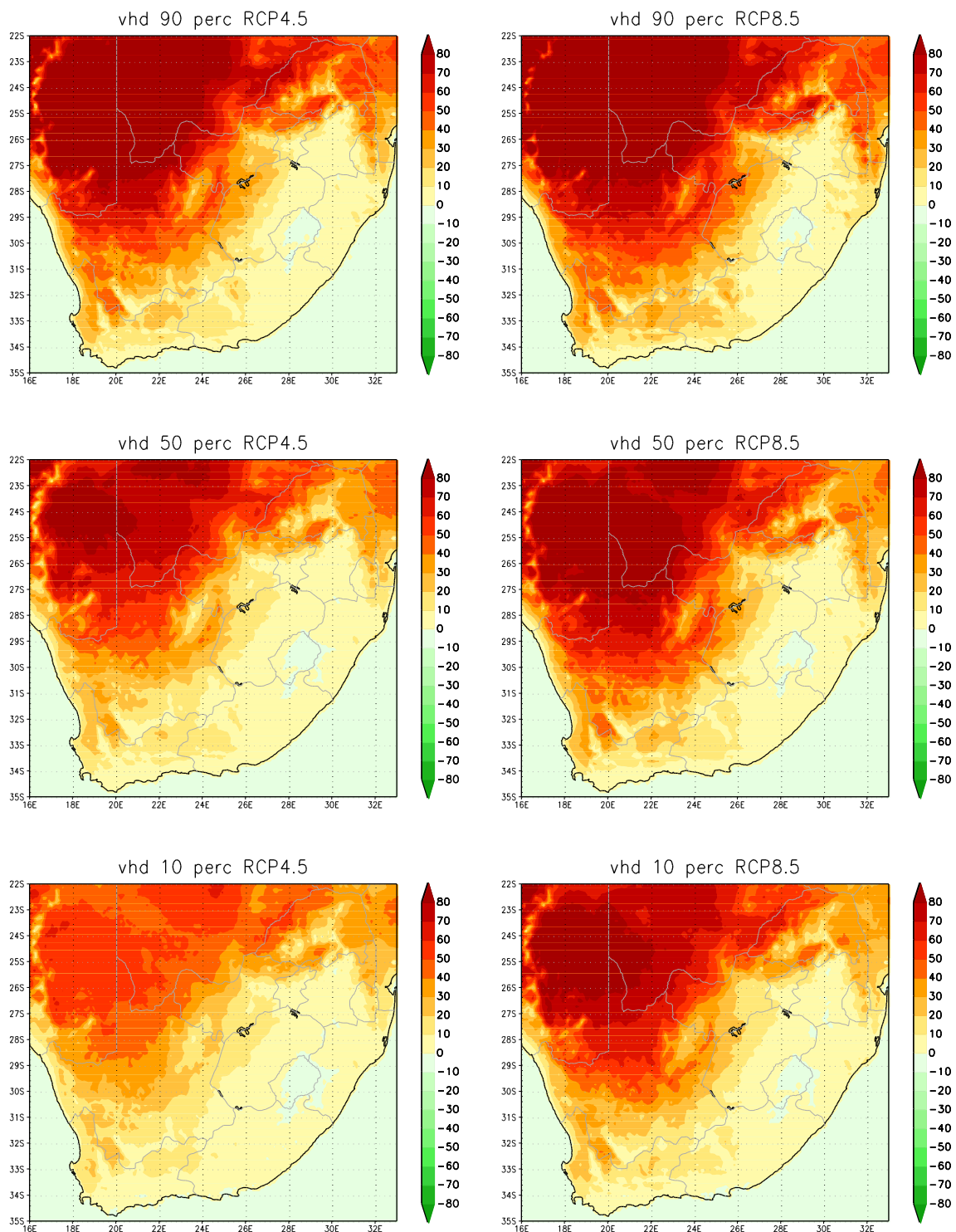


Figure 11: CCAM projected change in the annual average number of very hot days (units are days per grid point per year) over South Africa at 8 km resolution, for the time-slab 2021-2050 relative to 1961-1990. The 10th, 50th and 90th percentiles are shown for the ensemble of downscalings of six GCM projections under RCP4.5 (left) and RCP8.5 (right).

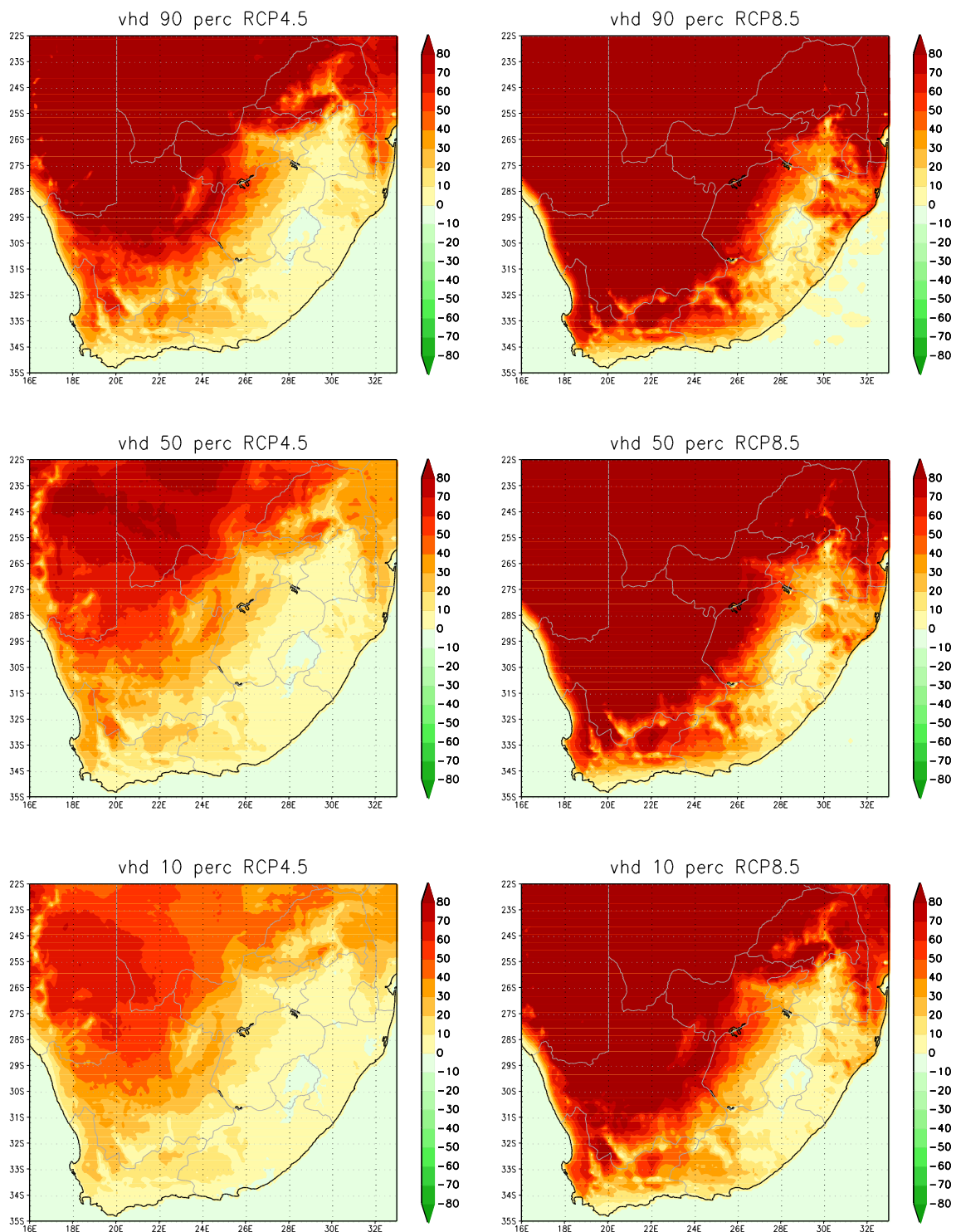


Figure 12: CCAM projected change in the annual average number of very hot days (units are days per grid point per year) over South Africa, for the time-slab 2071-2100 relative to 1961-1990. The 10th, 50th and 90th percentiles are shown for the ensemble of downscalings of six GCM projections under RCP4.5 (left) and RCP8.5 (right).



3.5 Heat-wave days

The model-simulated annual-average numbers of heat-wave days (units are number of days per model grid point) are displayed in Figure 13, for the baseline period 1961-2000. A heat-wave is defined as an event when the maximum temperature at a specific location exceeds the average maximum temperature of the warmest month of the year at that location by 5 °C, for a period of at least three days. The total number of days occurring within a heat-wave is referred to as “heat-wave days”.

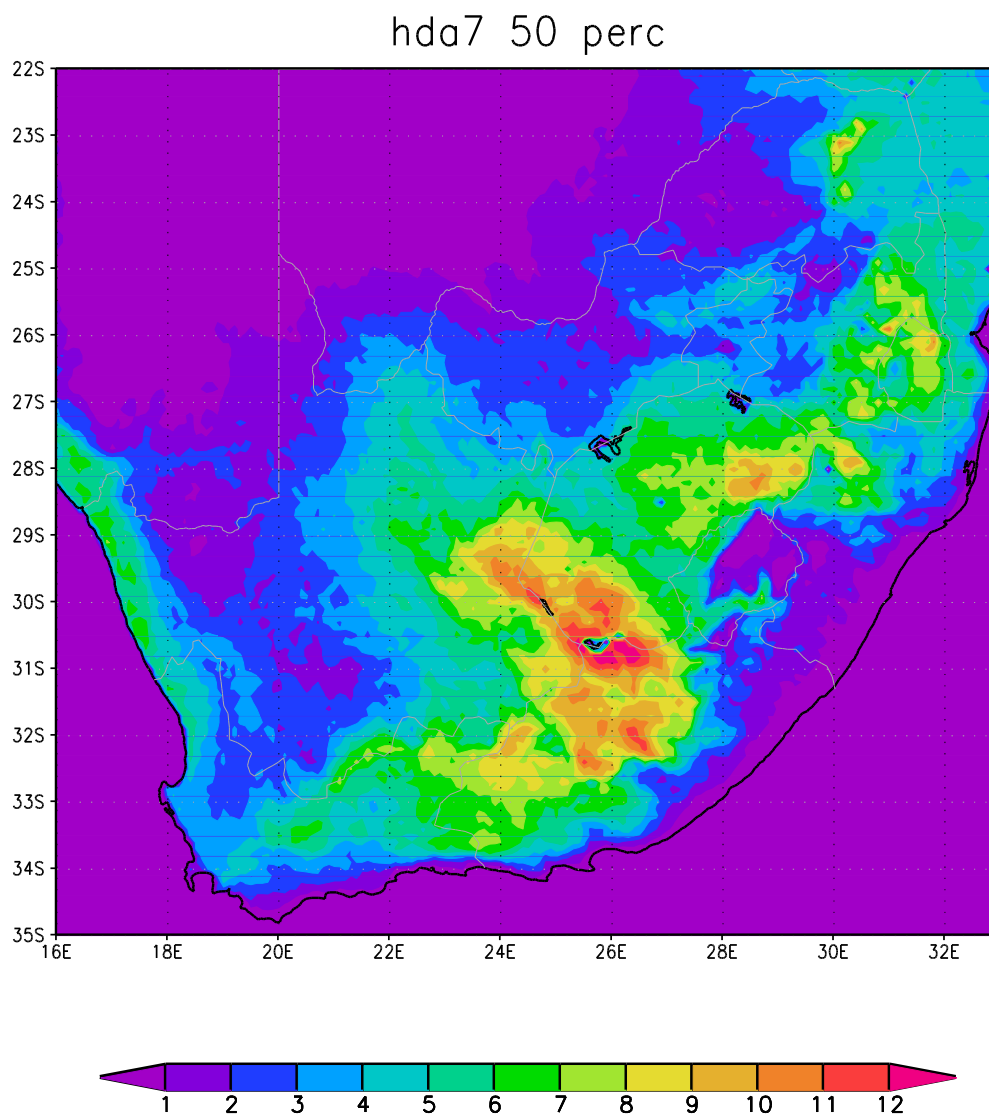


Figure 13: CCAM simulated annual average number of heat-wave days (units are number of days per grid point per year) over South Africa at 8 km resolution, for the baseline period 1961-1990. The median of simulations is shown for the ensemble of downscalings of six GCM simulations.



In association with drastically rising maximum temperatures (Figure 14), the frequency of occurrence of heat-wave days are also projected to increase drastically under climate change. For the period 2021-2050 relative to 1961-1990, under low mitigation, heat-wave days are projected to increase with more than 10-20 days per year over most of the country (Figure 14). Larger increases of more than 20 days per year may plausibly occur over parts of North West and the Northern Cape. Even under high mitigation, the increase in the number of heat-wave days may be 10-20 or more over the interior regions of eastern South Africa with larger increases plausible over the western interior regions (Figure 14).

For the period 2070-2099 relative to 1961-1990 under low mitigation, heat-wave days are projected to increase drastically, with 80 or more days per year being heat wave days over much of the interior (Figure 15). Significantly less drastic increases are projected under modest-high mitigation, although increases by as many as 40 days remain plausible over the Northern Cape and North West (Figure 15).

Increases in the occurrence of heat-wave days occur in association with projected changes in the frequency of very hot days and high fire-danger days (see section 3.4 and 3.6). Since heat-wave days are associated with prolonged periods of oppressive temperatures, these changes may impact on human and animal health through increased heat stress, are likely to impact negatively on crop yield and are plausible to be conducive to the occurrence of veld and forest fires.

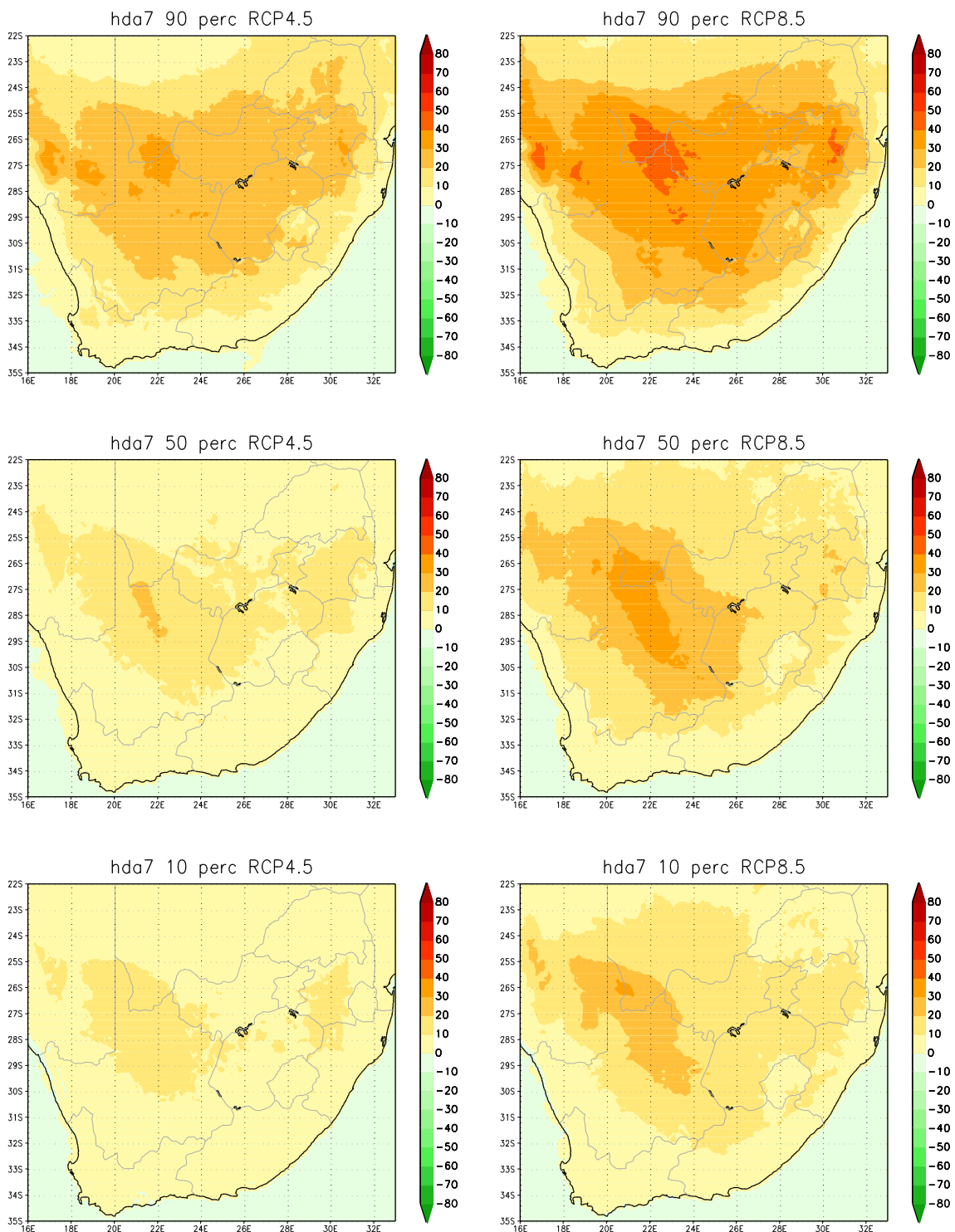


Figure 14: CCAM projected change in the annual average number of heat-wave days (units are number of days per grid point per year) over South Africa, for the time-slab 2021-2050 relative to 1961-1990. The 10th, 50th and 90th percentiles are shown for the ensemble of downscalings of six GCM projections under RCP4.5 (left) and RCP8.5 (right).

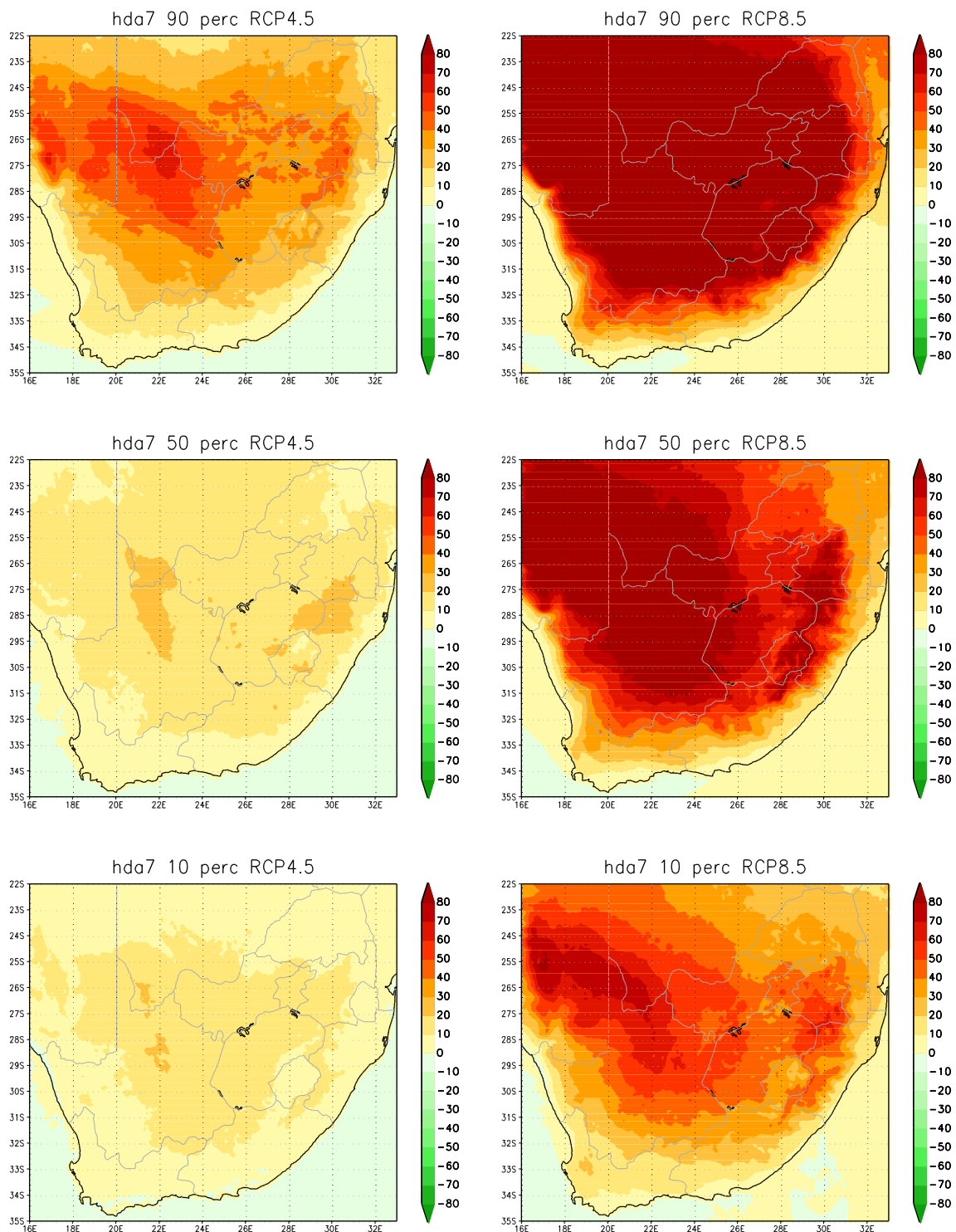


Figure 15: CCAM projected change in the annual average number of heat-wave days (units are number of days per grid point per year) over South Africa, for the time-slab 2071-2100 relative to 1961-1990. The 10th, 50th and 90th percentiles are shown for the ensemble of downscalings of six GCM projections under RCP4.5 (left) and RCP8.5 (right).



3.6 High fire-danger days

The model-simulated annual average number of high fire-danger days (days when the McArthur Fire Danger Index exceeds a value of 24 - units are number of days per model grid point) are displayed in Figure 16 for the baseline period 1961-2000. Over much of the grasslands of central South Africa and the forested areas of eastern South Africa, about 20 high fire-danger days occur on average per year.

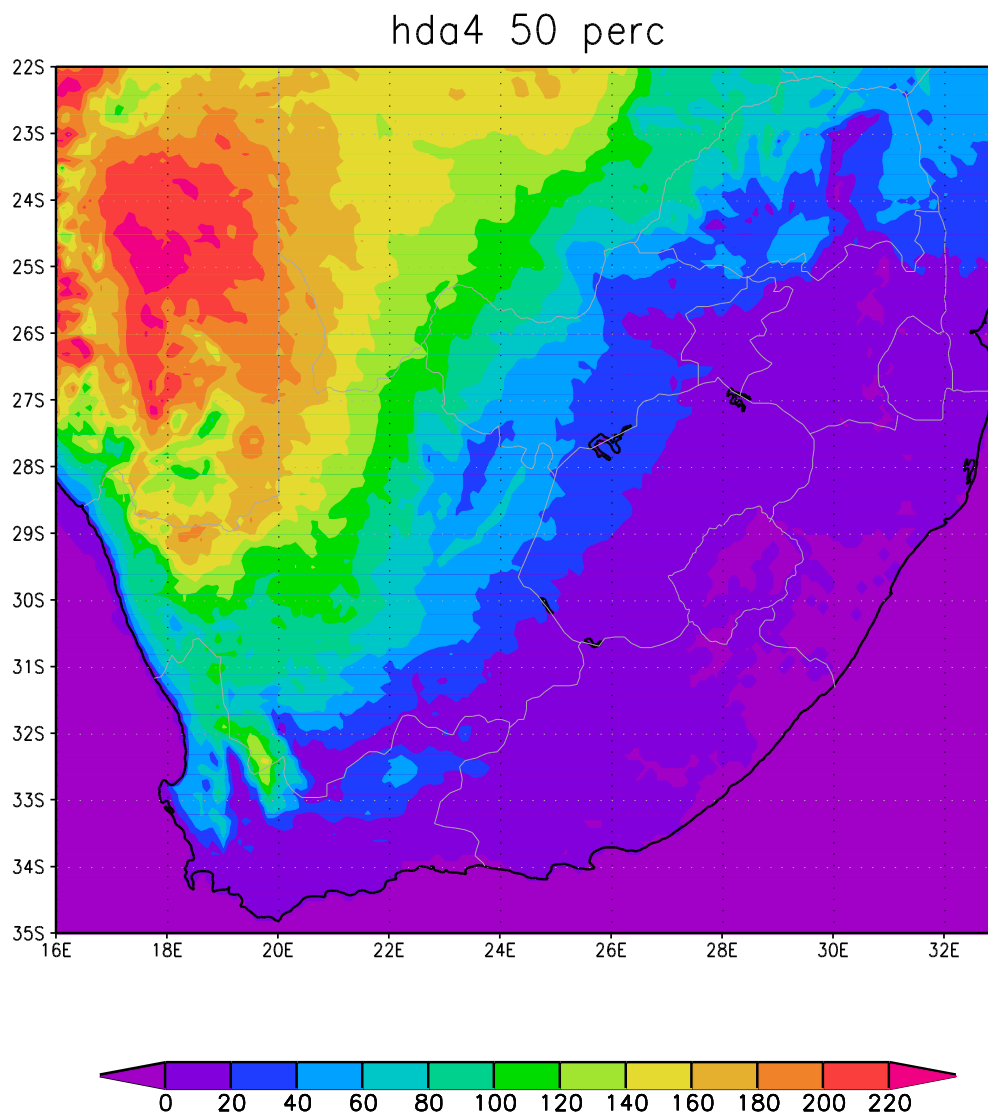


Figure 16: CCAM simulated annual average number of high fire-danger days (units are number of days per grid point per year) over South Africa, for the baseline period 1961-1990. The median of simulations is shown for the ensemble of downscalings of six GCM simulations.

In association with drastically rising maximum temperatures (Figures 5 and 6), the frequency of occurrence of high fire-danger days are also projected to increase drastically under climate change (Figure 17). For the period 2021-2050 relative to 1961-1990, under low mitigation,



high fire-danger days are projected to increase with as many as 10-30 days per year in the forested regions of Mpumalanga and Limpopo. Somewhat larger increases are projected for the central grasslands and the western parts of the domain (Figure 17). Even under modest-high mitigation, the increase in the number of high fire-danger days may be as many as 10-30 over eastern interior, with larger increases plausible over the western interior (Figure 17).

For the period 2070-2099 relative to 1961-1990, under low mitigation, high fire-danger days are projected to increase with as many as 50 to more than 80 days per year over the western part of the domain, including the Free State grasslands (Figure 18). Under modest-high mitigation, the increase in the number of high fire-danger days may be as many as 40-80 over the western interior, but with significantly smaller increases projected for the central grasslands and the forested regions in the east (Figure 18). Increases in the occurrence of high fire-danger days occur in association with projected changes in the frequency of occurrence of very hot days and heat-wave days (see sections 3.4 and 3.5).

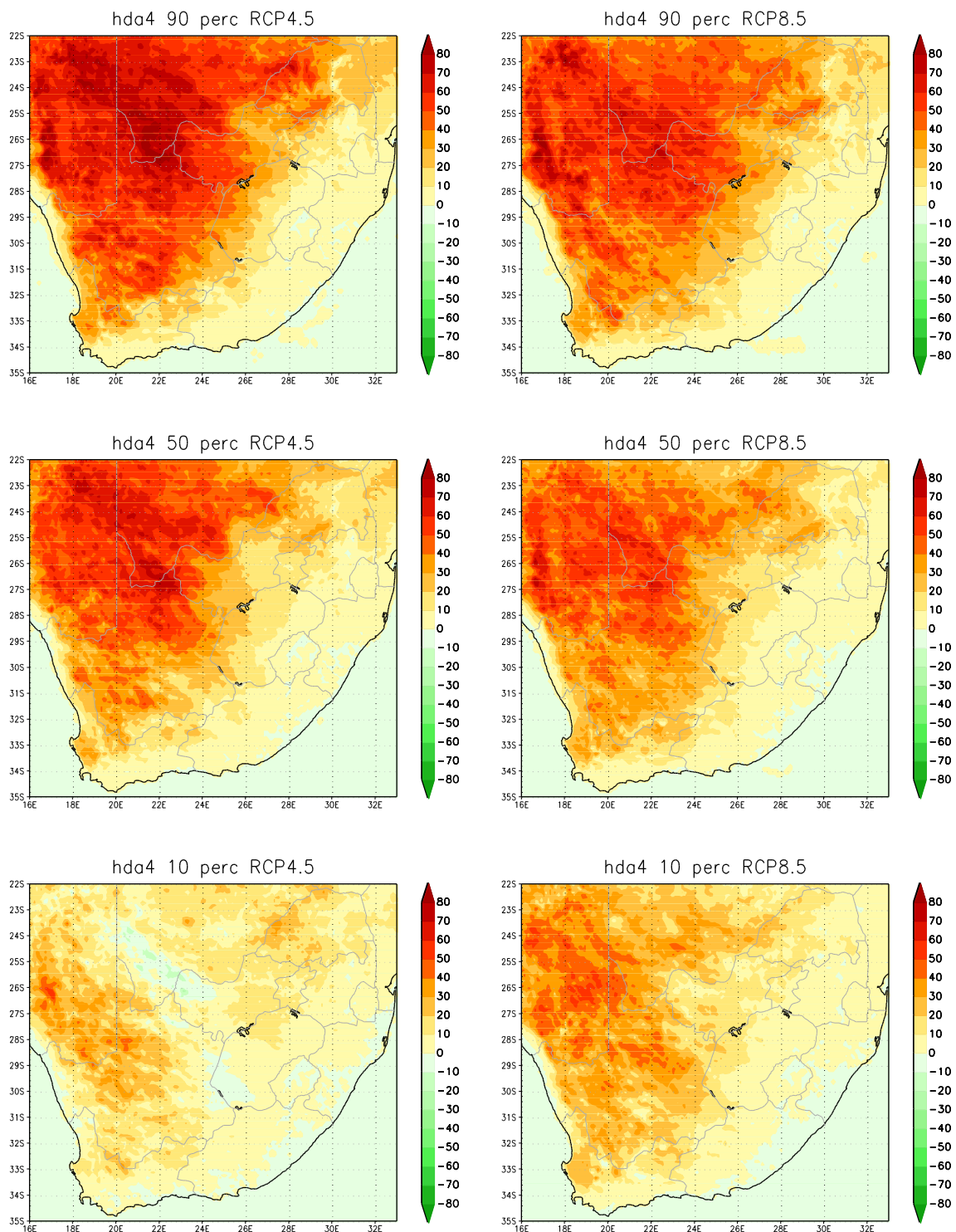


Figure 17: CCAM projected change in the annual average number of high fire-danger days (units are number of days per grid point per year) over South Africa, for the time-slab 2021-2050 relative to 1961-1990. The 10th, 50th and 90th percentile are shown for the ensemble of downscalings of six GCM projections under RCP4.5 (left) and RCP8.5 (right).

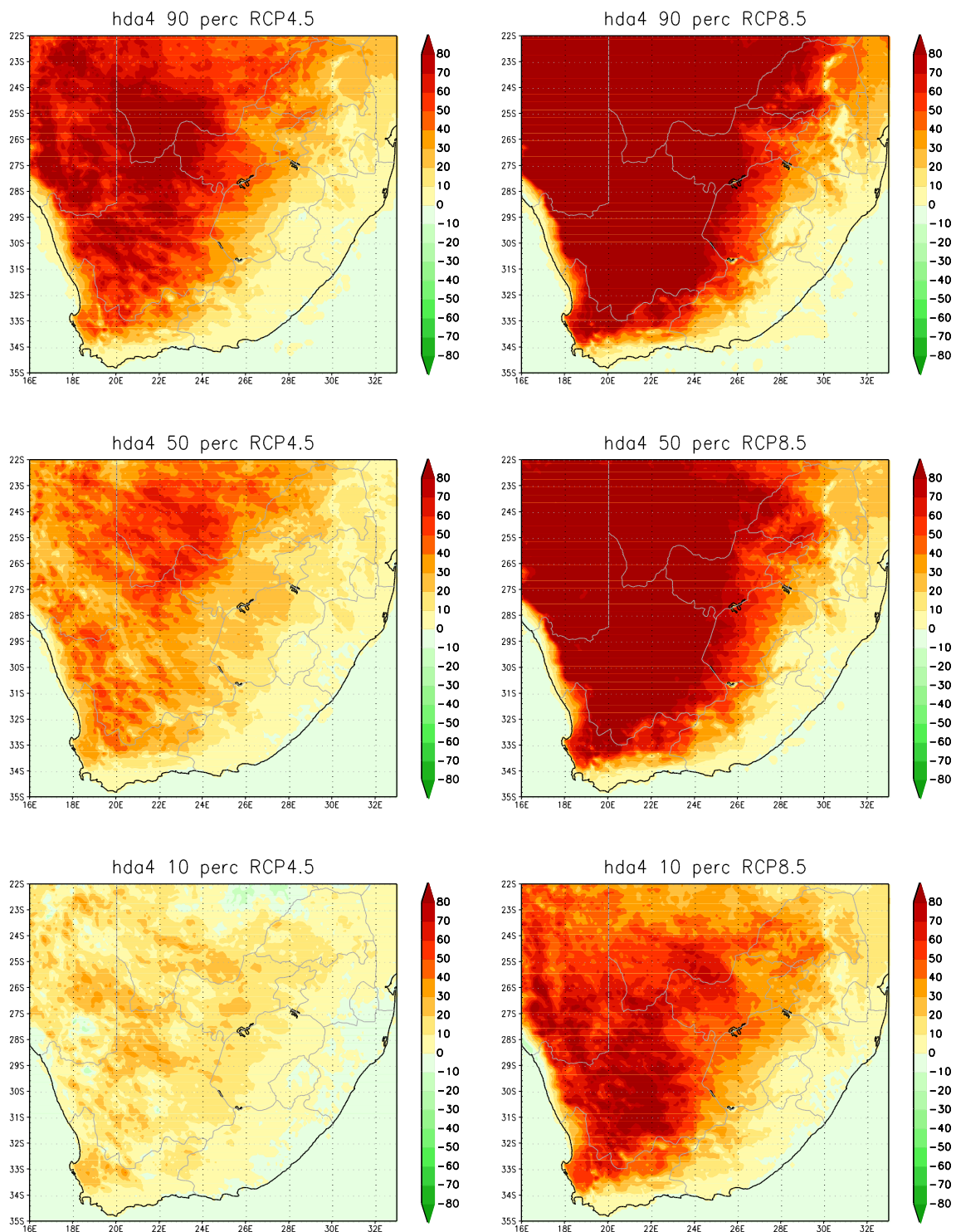


Figure 18: CCAM projected change in the annual average number of high fire-danger days (units are number of days per grid point per year) over South Africa, for the time-slab 2071-2100 relative to 1961-1990. The 10th, 50th and 90th percentile are shown for the ensemble of downscalings of six GCM projections under RCP4.5 (left) and RCP8.5 (right).

3.7 Rainfall

The model-simulated annual average rainfall totals (mm) are displayed in Figure 19, for the baseline period 1961-2000. There is a pronounced west-east rainfall gradient over the country. Over the eastern escarpment and east coast the simulated annual rainfall totals exceed 1000 mm.

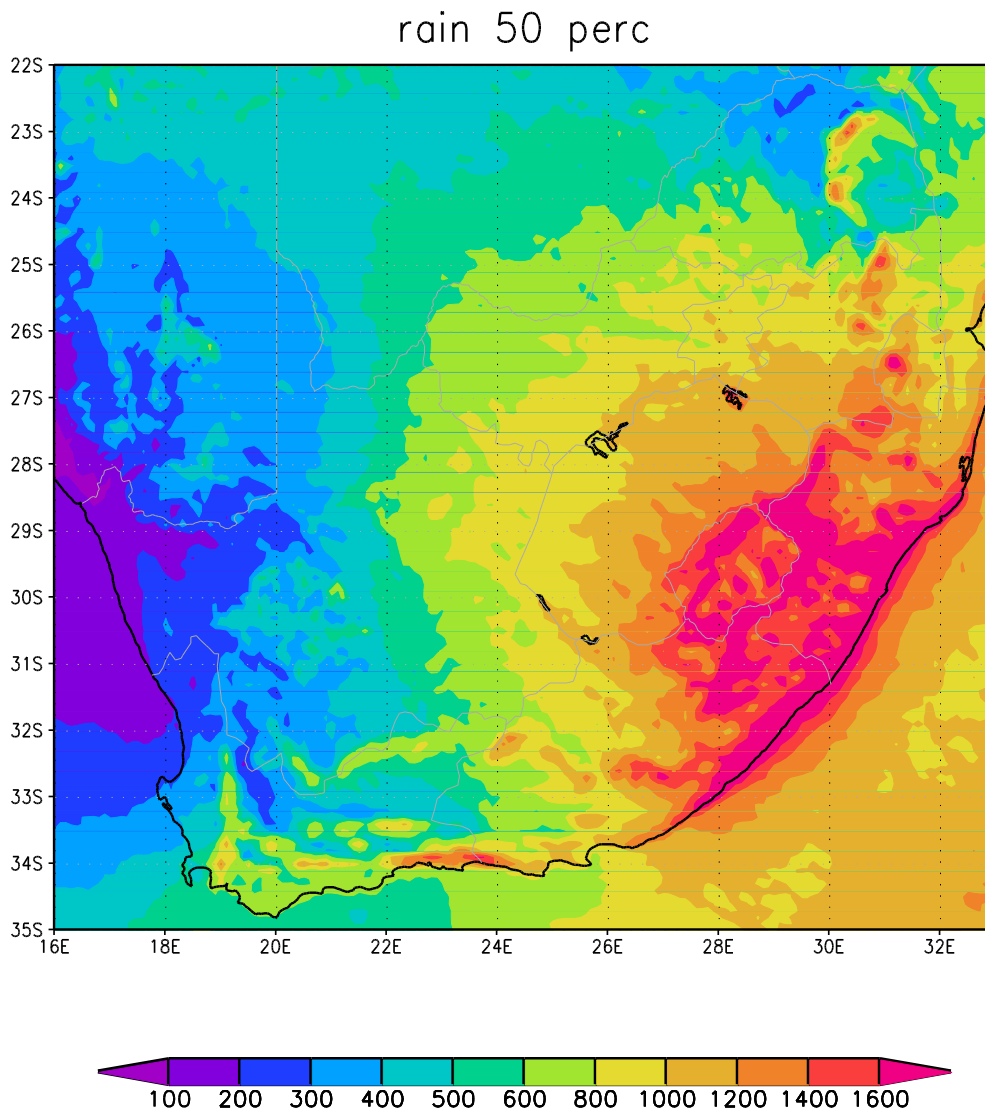


Figure 19: CCAM simulated annual average rainfall totals (mm) over eastern South Africa, for the baseline period 1961-1990 at 8 km resolution. The median of simulations is shown for the ensemble of downscalings of six GCM simulations.

A general decrease in rainfall is plausible over southern Africa under enhanced anthropogenic forcing (Christensen et al., 2007; Engelbrecht et al., 2009).



For the period 2021-2050 relative to the period 1971-2000, under low mitigation, rainfall is projected to increase over the central interior and the east coast. A minority of ensemble members project general rainfall increases over eastern South Africa (Figure 20). The western interior, northeastern parts and the winter rainfall region of the southwestern Cape are projected to become generally drier by most ensemble members.

The projected changes in rainfall patterns under high mitigation are very similar to the patterns projected under low mitigation (Figure 21). For the period 2070-2099 relative to the period 1961-1990, under low mitigation, rainfall is projected to decrease over the central interior and east coast of South Africa by most ensemble members (Figure 21). In fact, the pattern of change closely resembles that of the 2021-2050 period. A minority of ensemble members project general rainfall increases over eastern South Africa, but most ensemble members project rainfall decreases over the western parts of the country (Figure 21). The projected changes in rainfall patterns for 2070-2099 under high mitigation is very similar to the patterns projected under low mitigation (Figure 21).

The projected changes in rainfall patterns over South Africa in the ensemble of downscalings described here, and more generally in AR4 and AR5 projections, display more uncertainty than in the case of projected changes in temperature. This implies that adaptation policy makers need to take into account a range of different rainfall futures, often of different signal (i.e. drier and wetter) during the decision making process.

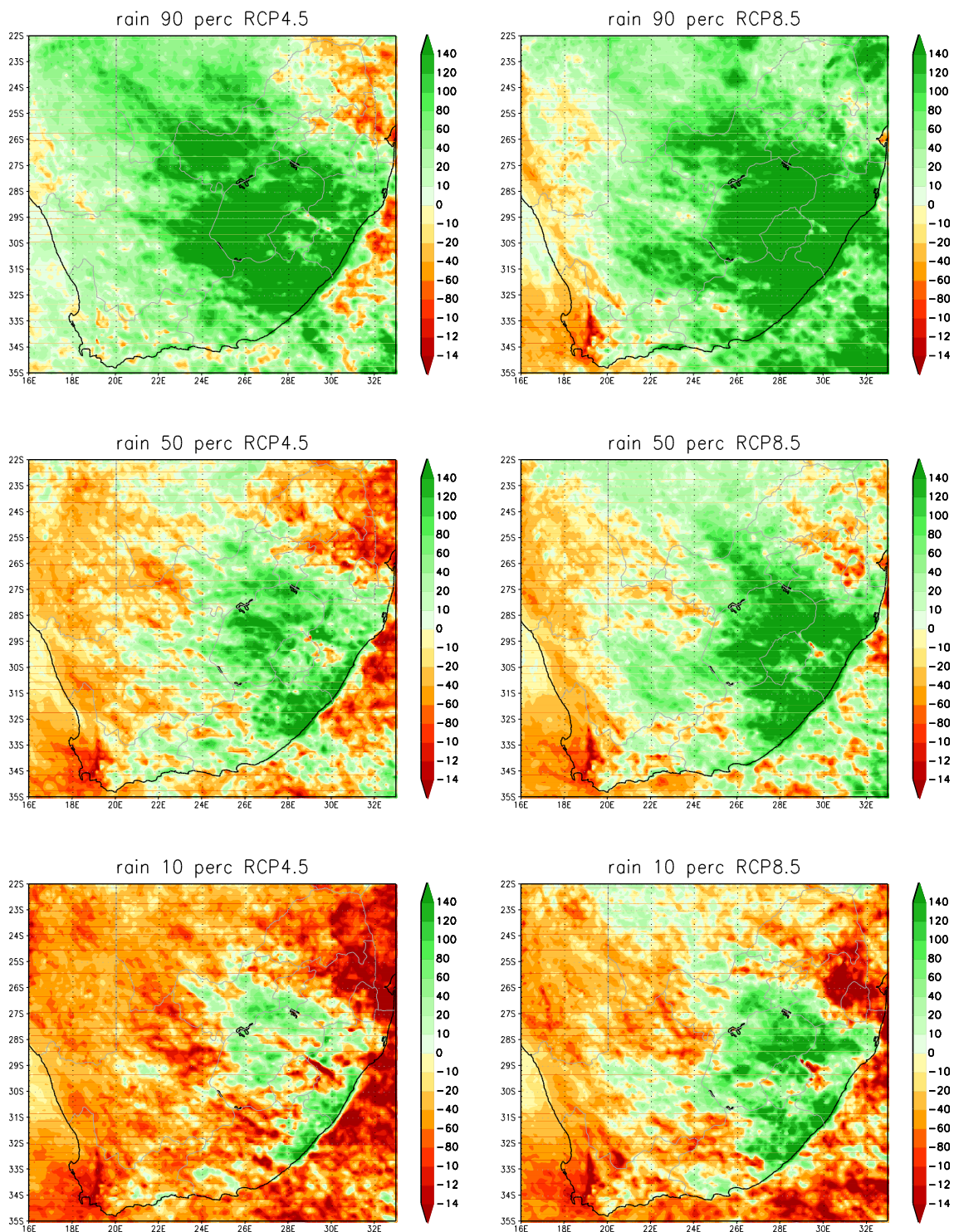


Figure 20: CCAM projected change in the annual average rainfall totals (mm) over eastern South Africa at 8 km resolution, for the time-slab 2021-2050 relative to 1961-1990. The 10th, 50th and 90th percentiles are shown for the ensemble of downscalings of six GCM projections under RCP4.5 (left) and RCP8.5 (right).

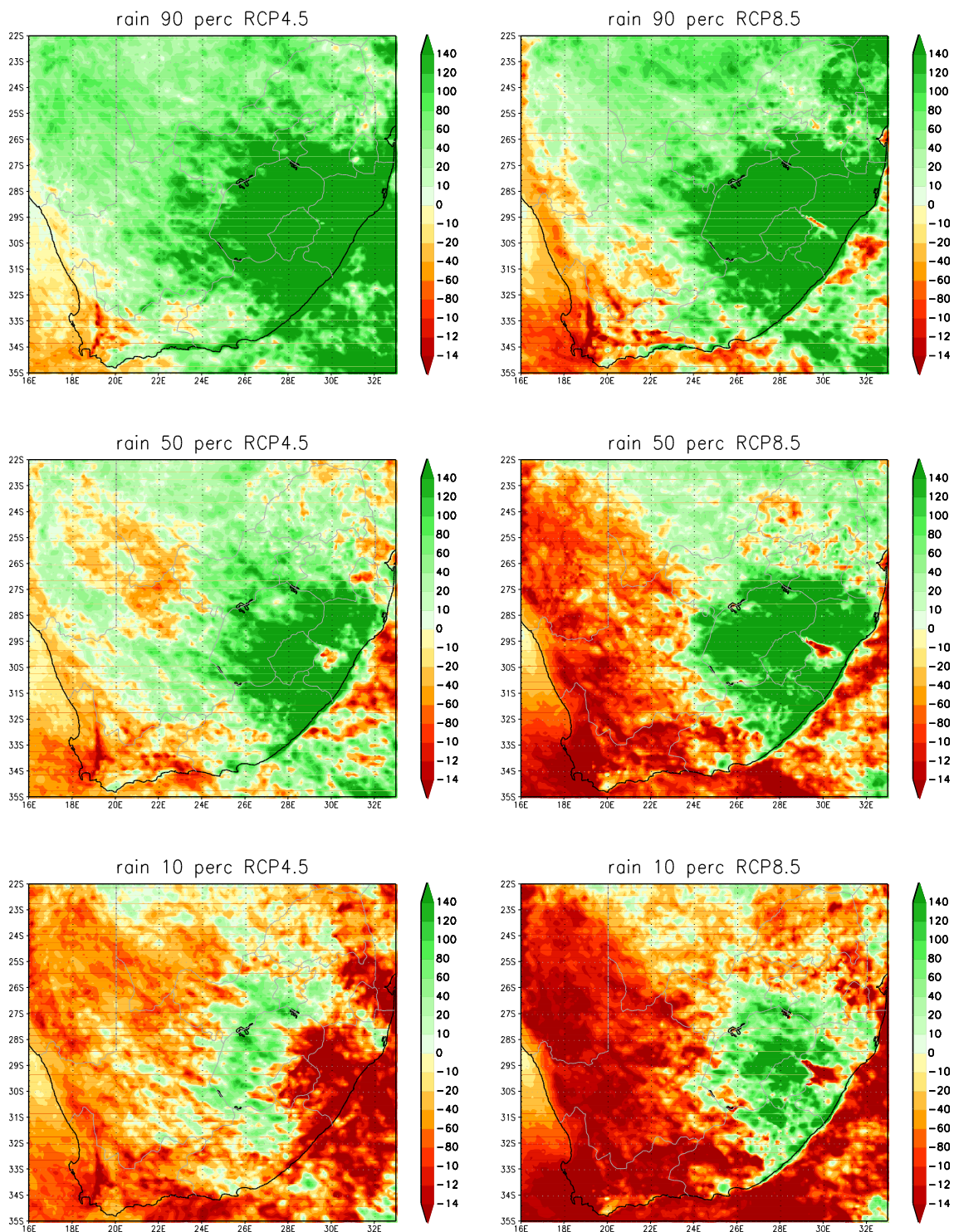


Figure 21: CCAM projected change in the annual average rainfall totals (mm) over eastern South Africa, for the time-slab 2071-2100 relative to 1961-1990. The 10th, 50th and 90th percentiles are shown for the ensemble of downscalings of six GCM projections under RCP4.5 (left) and RCP8.5 (right).



3.8 Extreme rainfall events (including severe thunderstorms and lightning)

The model-simulated annual average extreme rainfall event frequencies (units are number of events per model grid box per year) are displayed in Figure 22, for the baseline period 1971-2000. Here an extreme rainfall event is defined as 20 mm of rain occurring within 24 hours over an area of 64 km²). Over the east coast and eastern escarpment regions more than 10 extreme rainfall events are simulated to occur annually, on the average.

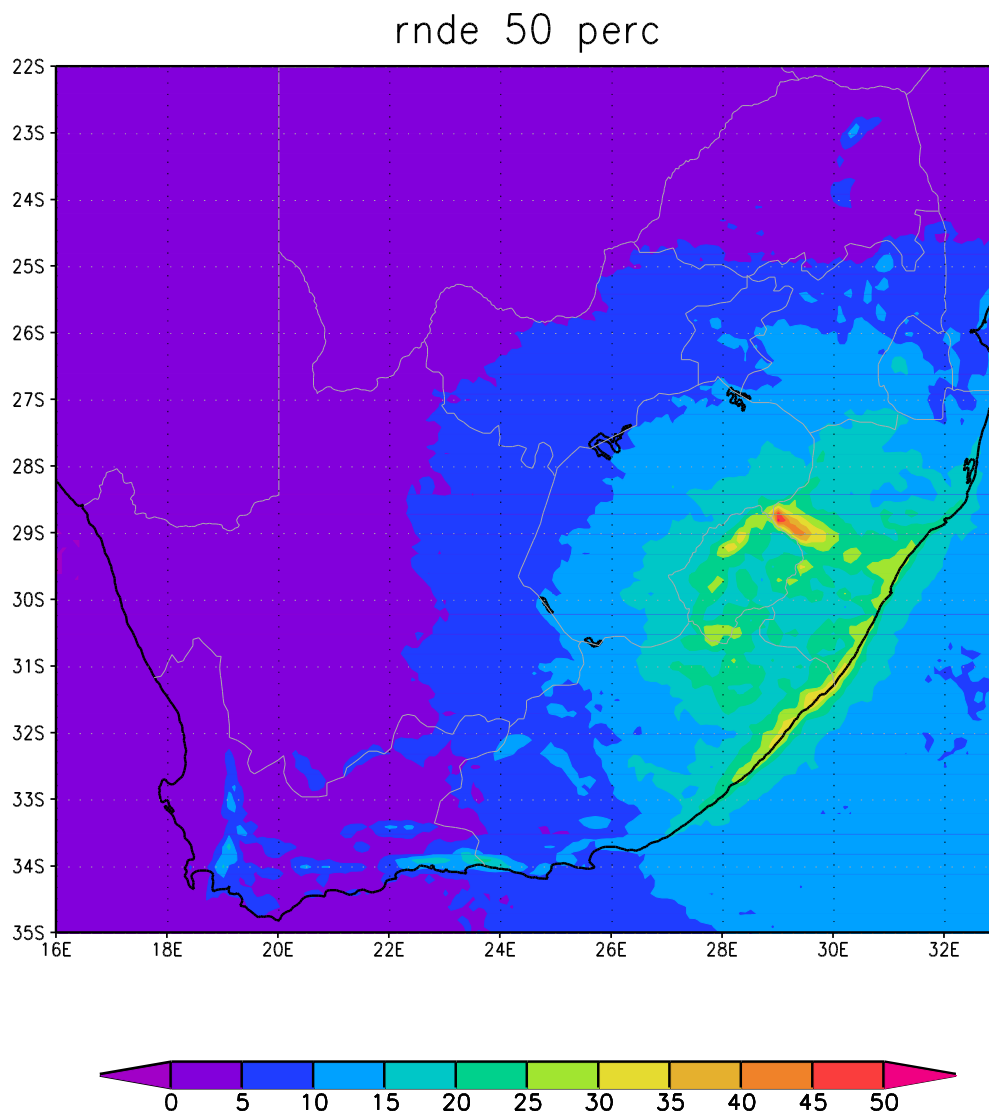


Figure 22: CCAM simulated annual average number of extreme rainfall days (units are number of days per grid point per year) over South Africa, for the baseline period 1961-1990. The median of simulations is shown for the ensemble of downscalings of six GCM simulations.



Consistent with the projected decreases in rainfall, extreme rainfall events are projected to increase in frequency over most of the central interior and east coast of South Africa under low mitigation, for the period 2021-2050 relative to 1961-1990, by most ensemble members (Figure 23). A minority of ensemble members project increases in extreme rainfall events over most of eastern South Africa (Figure 23).

Extreme rainfall events are also projected to decrease in frequency over most of eastern South Africa for the period 2070-2099, with the patterns of change very similar for the cases of low and high mitigation (Figure 24). A minority of ensemble members project increases in extreme rainfall events over most of eastern South Africa (Figure 24) for 2070-2099. The relatively large decreases in extreme rainfall events projected for Lesotho and the KwaZulu-Natal midlands may be important from the perspectives of run-off and water security.

The projected changes in extreme rainfall events under high mitigation are very similar to the patterns projected under low mitigation (Figures 23 and 24). Extreme rainfall events are mostly caused by intense thunderstorms, which are often also the cause of lightning, hail, damaging winds and flash floods. That is, the climate change projections analysed here are indicative that decreases in these hazardous storms are plausible over most of eastern South Africa, however, a minority of ensemble members are indicative of increases in such events. Adaptation policies therefore need to take into account the possibility that extreme rainfall events over eastern South Africa may increase in their frequency of occurrence.

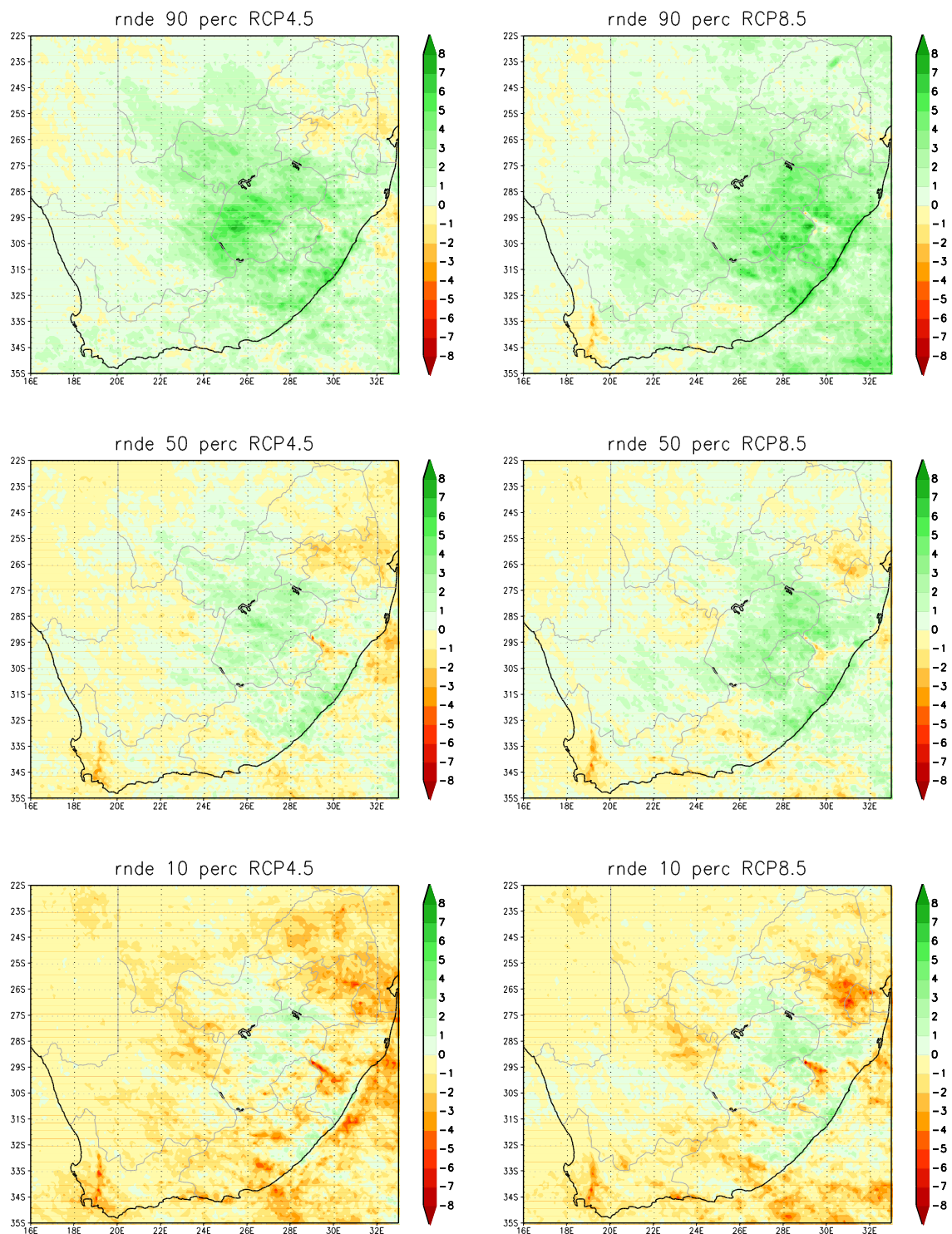


Figure 23: CCAM projected change in the annual average number of extreme rainfall days (units are numbers of grid points per year) over South Africa at 8 km resolution, for the time-slab 2021-2050 relative to 1961-1990. The 10th, 50th and 90th percentiles are shown for the ensemble of downscaleds of six GCM projections under RCP4.5 (left) and RCP8.5 (right).

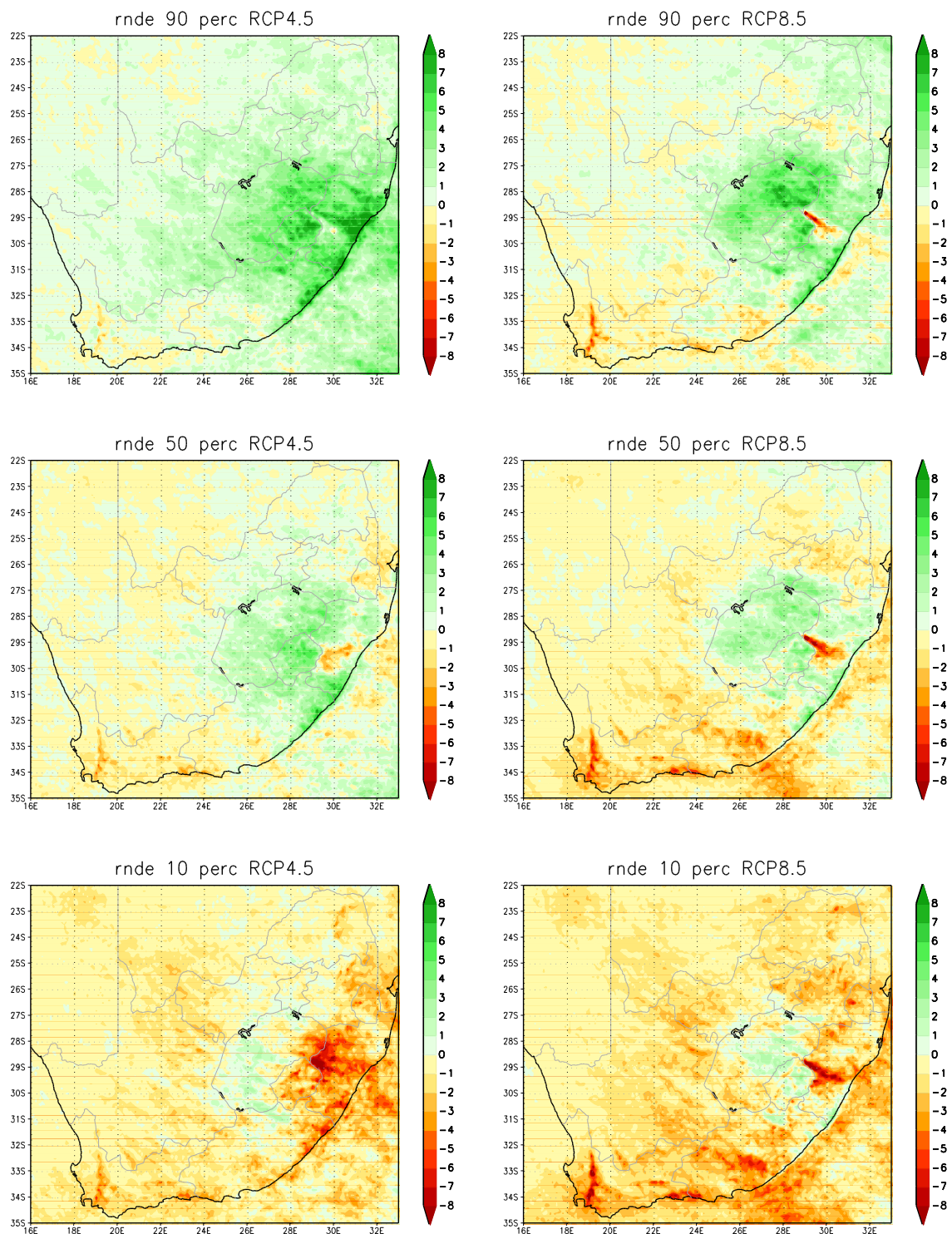


Figure 24: CCAM projected change in the annual average number of extreme rainfall days (units are numbers of grid points per year) over eastern South Africa, for the time-slab 2071-2100 relative to 1961-1990. The 10th, 50th and 90th percentiles are shown for the ensemble of downscaleds of six GCM projections under RCP4.5 (left) and RCP8.5 (right).

3.9 Wind speed

The model-simulated annual average wind speeds (m/s) are displayed in Figure 25, for the baseline period 1961-1990. The highest frequencies of strong-wind days occur along the east coast. The highest wind speeds are simulated to occur over the high-altitude regions of the eastern escarpment, extending along the southern escarpment to the mountains of the southwestern Cape. Portions of the interior of the Northern Cape are also simulated to experience high wind speeds on the average.

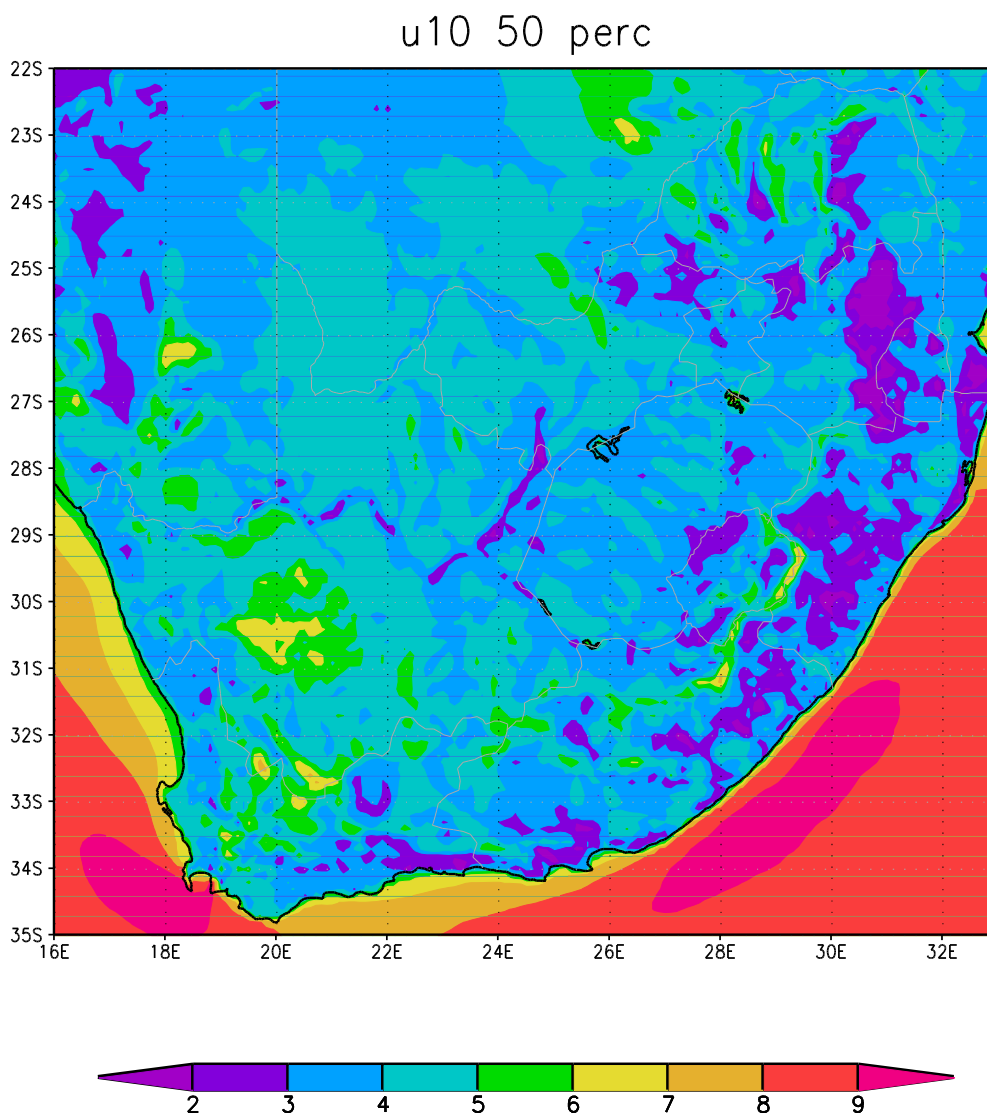


Figure 25: CCAM simulated average annual wind speed (m/s) over South Africa at 8 km resolution, for the baseline period 1961-1990. The median of simulations is shown for the ensemble of downscalings of six GCM simulations.

Most ensemble members are projecting reduced wind speeds for the southern interior regions for the period 2021-2050, relative to 1961-1990, in association with a poleward displacement



of the westerly wind regime under climate change (Figure 26). Associated decreases in wind-speed are projected over the Atlantic Ocean west of South Africa, in the region where the longshore southeasterly winds prevail. Most ensemble members project increases in wind speed for the northern interior regions (Figure 26). These changes are presumably occurring due to the strengthening of the continental heating under climate change.

These projected patterns of change are consistently projected across the mitigation scenarios and time-slabs 2021-2050 and 2070-2099 (Figures 26 and 27).

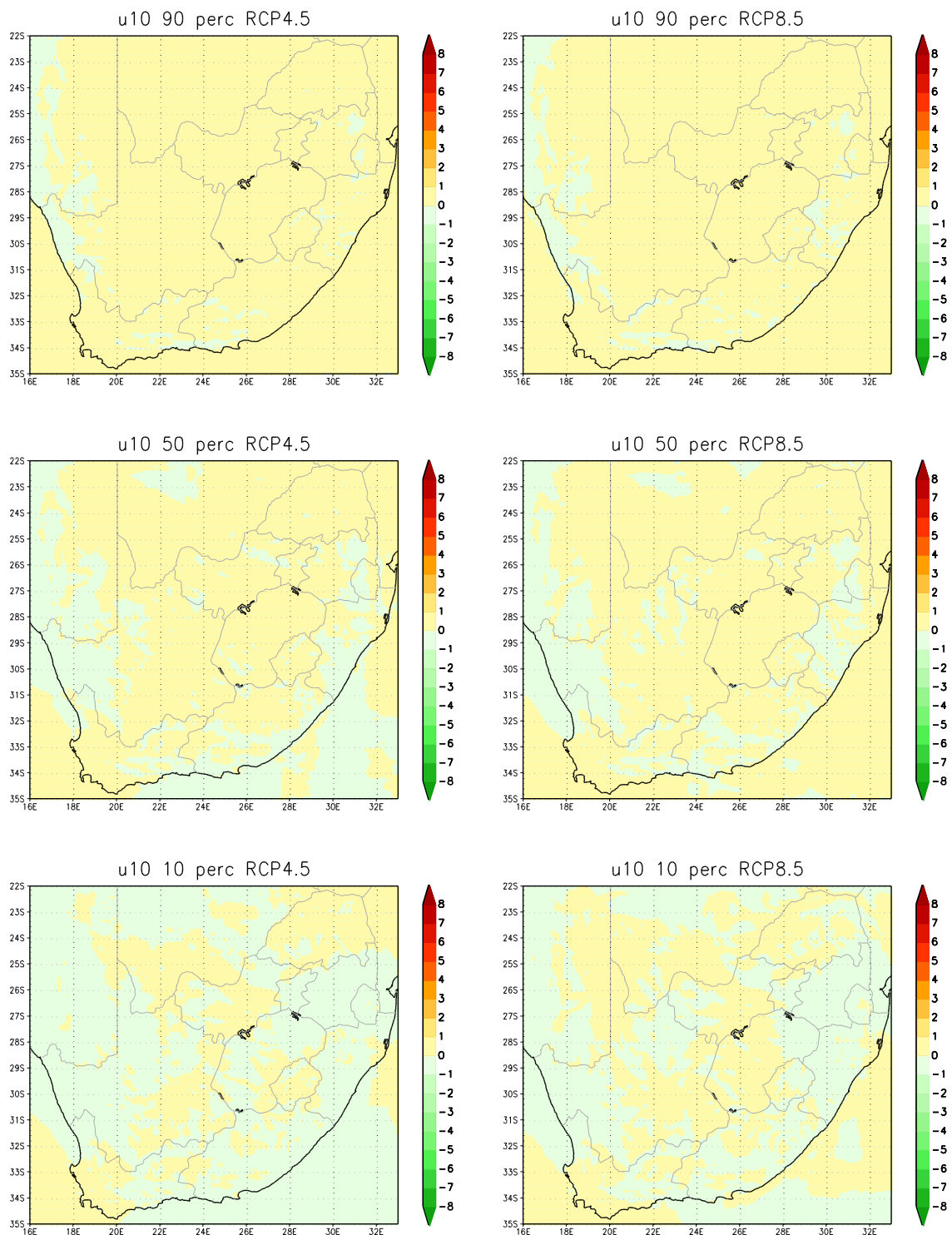


Figure 26: CCAM projected change in the annual average wind speed (m/s) over South Africa at 8 km resolution, for the time-slab 2021-2050 relative to 1961-1990. The 10th, 50th and 90th percentiles are shown for the ensemble of downscalings of six GCM projections under RCP4.5 (left) and RCP8.5 (right)

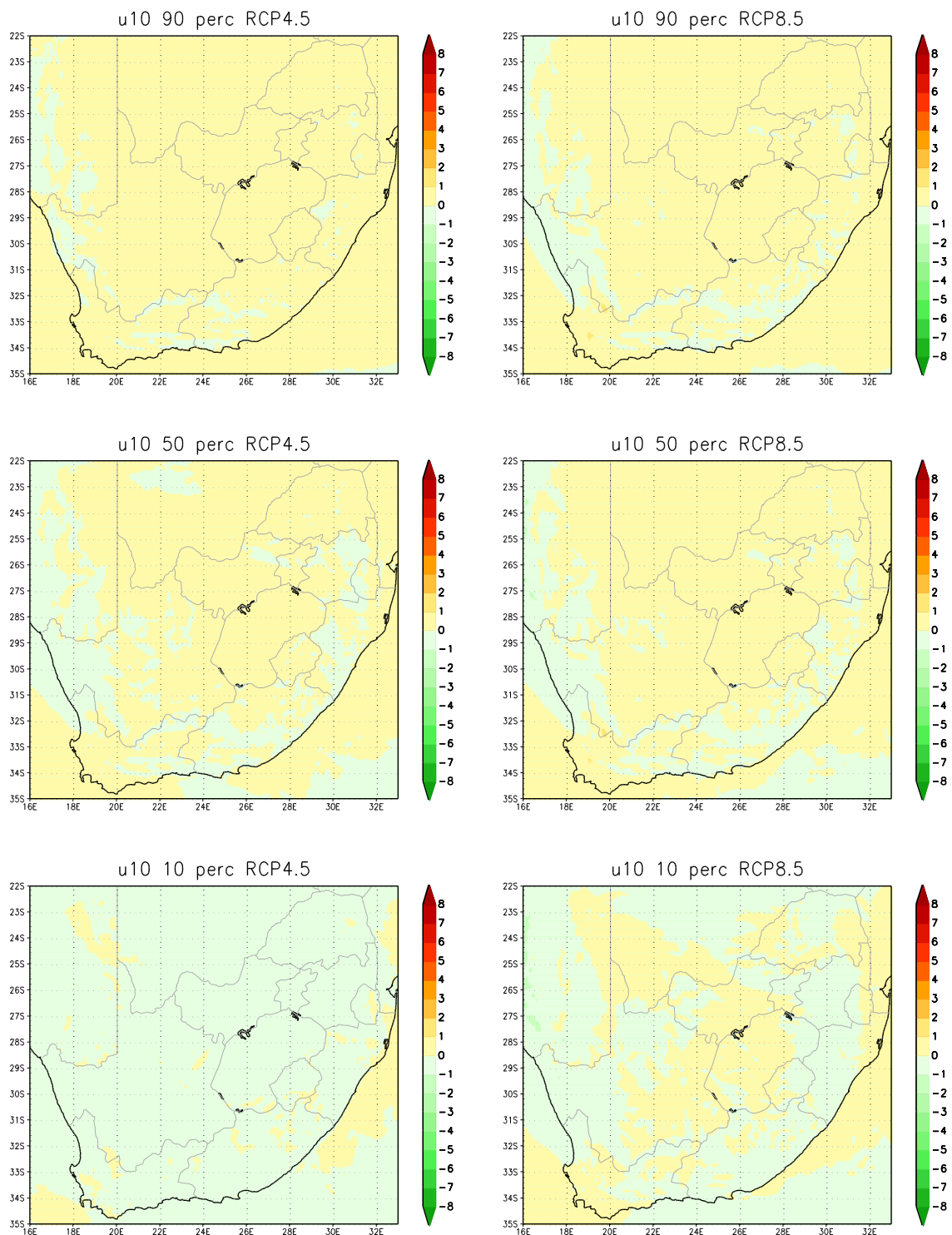


Figure 27: CCAM projected change in the annual average wind speed (m/s) over South Africa at 8 km resolution, for the time-slab 2091-2100 relative to 1961-1990. The 10th, 50th and 90th percentiles are shown for the ensemble of downscalings of six GCM projections under RCP4.5 (left) and RCP8.5 (right).



4 CONCLUSIONS

This report is based on an ensemble of high-resolution projections of future climate change over Africa, obtained by using the regional climate model CCAM to downscale the output of a number of CMIP5 (AR5) GCMs over Africa. The projections downscaled represent both high (RCP4.5) and low (RCP8.5) mitigation scenarios. CCAM was applied at 50 km resolution globally, and the experimental design of the simulations is consistent with that of CORDEX. The 50 km resolution global simulations were subsequently downscaled to a resolution of 8 km over South Africa. These projections are the most detailed yet obtained for South Africa. Many regional climate features, such as the high precipitation totals induced by the northern extension of the Drakensberg Mountain in Limpopo and the mountains of the southwestern Cape, and the high maximum temperatures that occur in the Orange and Limpopo river basins, are well represented. These features are not well resolved in the corresponding 50 km simulations, implying that the projected climate change signal, to the extent that it relates to topography, is more reliably described in the 8 km resolution simulations.

The 8 km resolution projections are indicative of drastic temperature increases in near-surface temperatures and related extreme events over South Africa. Already for the mid-future period of 2021-2050, high fire-danger days, heat-wave days and very hot days are likely to occur at unprecedented frequencies in South Africa. The projected changes are similar for low (RCP8.5) and modest-high (RCP4.5) mitigation futures. The changes may reach devastating proportions by the far-future period (2071-2099) under low mitigation futures, at least in terms of impacts on agriculture and livestock over the western interior and the Limpopo basin. However, the modelling indicates that under modest-high mitigation, changes in temperature and related extremes are significantly mitigated for the far-future period. The projections also provide evidence of a plausible increase in extreme convective rainfall events over the central interior regions under climate change, which implies associated increases in lightning frequencies. Associated increases in streamflow may benefit water yield in the mega-dam region.



5 REFERENCES

- Christensen JH, Hewitson B, Busuioc A, Chen A, Gao X, Held I, Jones R, Kolli RK, Kwon W-T, Laprise R, Magana Rueda V, Mearns L, Menendez CG, Raisanen J, Rinke A, Sarr A, Whetton P (2007). Regional climate projections. In: Solomon S, Qin D, Manning M, Chen Z, Marquis M, Averyt, AB, Tignor M, Miller HL (eds). *Climate change 2007: the physical science basis. Contribution of Working Group I to the Fourth Assessment Report of the Inter-governmental Panel on Climate Change*. Cambridge University Press, Cambridge.
- Engelbrecht CJ, Engelbrecht FA and Dyson LL (2013). High-resolution model projected changes in mid-tropospheric closed-lows and extreme rainfall events over southern Africa. *Int J Climatol* 33 173–187. doi:10.1002/joc.3420.
- Engelbrecht F, Adegoke J, Bopape MM, Naidoo M, Garland R, Thatcher M, McGregor J, Katzfey J, Werner M, Ichoku C and Gatebe C (2015). Projections of rapidly rising surface temperatures over Africa under low mitigation. *Environmental Research Letters*.
- Engelbrecht FA, Landman WA, Engelbrecht CJ, Landman S, Bopape MM, Roux B, McGregor JL and Thatcher M (2011). Multi-scale climate modelling over Southern Africa using a variable-resolution global model. *Water SA* 37 647–658.
- Engelbrecht FA, McGregor JL and Engelbrecht CJ (2009). Dynamics of the conformal-cubic atmospheric model projected climate-change signal over southern Africa. *Int J Climatol* 29 1013–1033.
- James R and Washington R (2013). Changes in African temperature and precipitation associated with degrees of global warming. *Climatic Change* 117 859–872. DOI 10.1007/s10584-012-0581-7.
- Katzfey KK, McGregor JM, Nguyen K and Thatcher M (2009). Dynamical downscaling techniques: Impacts on regional climate change signals. 18th World IMACS/MODSIM Congress, Cairns, Australia, July 2009.
- Kowalczyk EA, Garratt JR and Krummel PB (1994). Implementation of a soil-canopy scheme into the CSIRO GCM -regional aspects of the model response. CSIRO Div. Atmospheric Research Tech. Paper No. 32. 59 pp



- LTAS (2013). Climate trends and scenarios for South Africa. Long-term Adaptation Scenarios Flagship Research Programme (LTAS). Phase 1, Technical Report no 6, pp 1-37. Contributors Midgley G., Engelbrecht F.A., Hewitson B., Chris J., New M., Tadross M., Schlosser A. and Dr Kenneth Strzepek.
- Malherbe J, Engelbrecht FA and Landman WA (2013). Projected changes in tropical cyclone climatology and landfall in the Southwest Indian Ocean region under enhanced anthropogenic forcing. *Clim Dyn* 40 2867–2886.
- McGregor JL (2005). C-CAM: Geometric aspects and dynamical formulation. CSIRO Atmospheric Research Tech. Paper No 70, 43 pp.
- McGregor JL and Dix MR (2001). The CSIRO conformal-cubic atmospheric GCM. In: Hodnett PF (ed.) *Proc. IUTAM Symposium on Advances in Mathematical Modelling of Atmosphere and Ocean Dynamics*. Kluwer, Dordrecht. 197-202.
- McGregor J.L. and M.R. Dix (2001). The CSIRO conformal-cubic atmospheric GCM. In: Hodnett PF (ed.) *Proc. IUTAM Symposium on Advances in Mathematical Modelling of Atmosphere and Ocean Dynamics*. Kluwer, Dordrecht. 197-202.
- McGregor JL and Dix MR (2008). An updated description of the Conformal-Cubic Atmospheric Model. In: Hamilton K and Ohfuchi W (eds.) *High Resolution Simulation of the Atmosphere and Ocean*. Springer Verlag. 51-76.
- Niang I, Ruppel OC, Abdrabo M, Essel A, Lennard C, Padgham J, Urquhart P, Adelekan I, Archibald S, Barkhordarian A, Battersby J, Balinga M, Bilir E, Burke M, Chahed M, Chatterjee M, Chidzie CT, Descheemaeker K, Djoudi H, Ebi KL, Fall PD, Fuentes R, Garland R, Gaye F, Hilmi K, Gbobaniyi E, Gonzalez P, Harvey B, Hayden M, Hemp A, Jobbins G, Johnson J, Lobell D, Locatelli B, Ludi E, Otto Naess L, Ndebele-Murisa MR, Ndiaye A, Newsham A, Njai S, Nkem, Olwoch JM, Pauw P, Pramova E, Rakotondrafara M-L, Raleigh C, Roberts D, Roncoli C, Sarr AT, Schleyer MH, Schulte-Uebbing L, Schulze R, Seid H, Shackleton S, Shongwe M, Stone D, Thomas D, Ugochukwu O, Victor D, Vincent K, Warner K, Yaffa S (2014). IPCC WGII AR5 Chapter 22 pp 1-115.
- Winsemius HC, Dutra E, Engelbrecht FA, Archer Van Garderen E, Wetterhall F, Pappenberger F and Werner MGF 2(014). The potential value of seasonal forecasts in a changing climate in southern Africa. *Hydrol. Earth Syst. Sci.* 18 1525–1538.